

Future temperature extremes threaten land vertebrates

<https://doi.org/10.1038/s41586-022-05606-z>

Gopal Murali^{1,2}✉, Takuya Iwamura^{3,4}, Shai Meiri^{5,6} & Uri Roll²

Received: 19 September 2021

Accepted: 28 November 2022

Published online: 18 January 2023

 Check for updates

The frequency, duration, and intensity of extreme thermal events are increasing and are projected to further increase by the end of the century^{1,2}. Despite the considerable consequences of temperature extremes on biological systems^{3–8}, we do not know which species and locations are most exposed worldwide. Here we provide a global assessment of land vertebrates' exposures to future extreme thermal events. We use daily maximum temperature data from 1950 to 2099 to quantify future exposure to high frequency, duration, and intensity of extreme thermal events to land vertebrates. Under a high greenhouse gas emission scenario (Shared Socioeconomic Pathway 5–8.5 (SSP5–8.5); 4.4 °C warmer world), 41.0% of all land vertebrates (31.1% mammals, 25.8% birds, 55.5% amphibians and 51.0% reptiles) will be exposed to extreme thermal events beyond their historical levels in at least half their distribution by 2099. Under intermediate-high (SSP3–7.0; 3.6 °C warmer world) and intermediate (SSP2–4.5; 2.7 °C warmer world) emission scenarios, estimates for all vertebrates are 28.8% and 15.1%, respectively. Importantly, a low-emission future (SSP1–2.6, 1.8 °C warmer world) will greatly reduce the overall exposure of vertebrates (6.1% of species) and can fully prevent exposure in many species assemblages. Mid-latitude assemblages (desert, shrubland, and grassland biomes), rather than tropics^{9,10}, will face the most severe exposure to future extreme thermal events. By 2099, under SSP5–8.5, on average 3,773 species of land vertebrates (11.2%) will face extreme thermal events for more than half a year period. Overall, future extreme thermal events will force many species and assemblages into constant severe thermal stress. Deep greenhouse gas emissions cuts are urgently needed to limit species' exposure to thermal extremes.

Anthropogenic climate change is exacerbating extreme thermal events, surpassing historical temperature records at an unprecedented rate^{2,11,12}. These extreme thermal events manifest as more frequent, intense, and prolonged episodes of extremely hot temperatures^{1,2} and are projected to increase further in the future^{2,12}. Recurring extreme thermal events directly affect biological functions, causing increased physiological stress, reduced reproductive output and population die-offs^{3–7}. Recent episodes of extremely hot temperatures have already resulted in widespread climate-change-induced population extirpations in many species^{3,4,6,13,14}. Such events will probably pose a considerable threat to biodiversity in the coming decades^{3–6,15}. Evaluating the impacts of extreme thermal events on biodiversity is therefore an urgent conservation priority in the face of rapid anthropogenic climate change^{16,17}.

There is increasing knowledge of the projected short-term extreme thermal events' effect on human health and agriculture^{18,19}. However, so far, studies on the effects of global climate change on biodiversity have largely focused on mean annual temperatures^{3,6,8,19–22}. Such approaches may capture chronic exposure to warming, but do not capture trends and effects of extreme thermal events—which are arguably

more important^{3,6,8}. First, animals experience, and are affected by, daily temperature and their fluctuations rather than long-term climates^{6,23}. Consequently, we need to account for short-term dynamics of heat stress that animals will experience in the future, such as how long or frequently they are exposed to extreme temperatures^{6,23–25}. Furthermore, spatial patterns of the severity of projected changes in extreme and mean temperatures are often mismatched^{26–29}. Finally, the frequency, duration, and intensity of extreme climatic events can arise due to increased temperature variability rather than by increased means^{30,31}. Thus, identifying the species and locations that will be most affected by short-term extreme thermal events is paramount.

Mechanistic and biophysical models that incorporate physiological and behavioural data offer great power to predict species' vulnerability to temperature extremes^{32,33}. However, such models cannot illuminate global trends across taxa because data on upper thermal tolerance are available only for a few hundred well-studied species³². Here we provide global insights into the impacts of extreme climates on land vertebrates by assessing species' geographical range exposure to future temperatures beyond their historical extreme temperatures as the baseline.

¹Jacob Blaustein Center for Scientific Cooperation, The Jacob Blaustein Institutes for Desert Research, Ben-Gurion University of the Negev, Midreshet Ben-Gurion, Israel. ²Mitrani Department of Desert Ecology, The Swiss Institute for Dryland Environments and Energy Research, The Jacob Blaustein Institutes for Desert Research, Ben-Gurion University of the Negev, Midreshet Ben-Gurion, Israel. ³Department F.-A. Forel for Aquatic and Environmental Sciences, Faculty of Science, University of Geneva, Geneva, Switzerland. ⁴Department of Forest Ecosystems and Society, College of Forestry, Oregon State University, Corvallis, OR, USA. ⁵School of Zoology, Tel Aviv University, Tel Aviv, Israel. ⁶The Steinhardt Museum of Natural History, Tel Aviv University, Tel Aviv, Israel. ✉e-mail: murali@post.bgu.ac.il

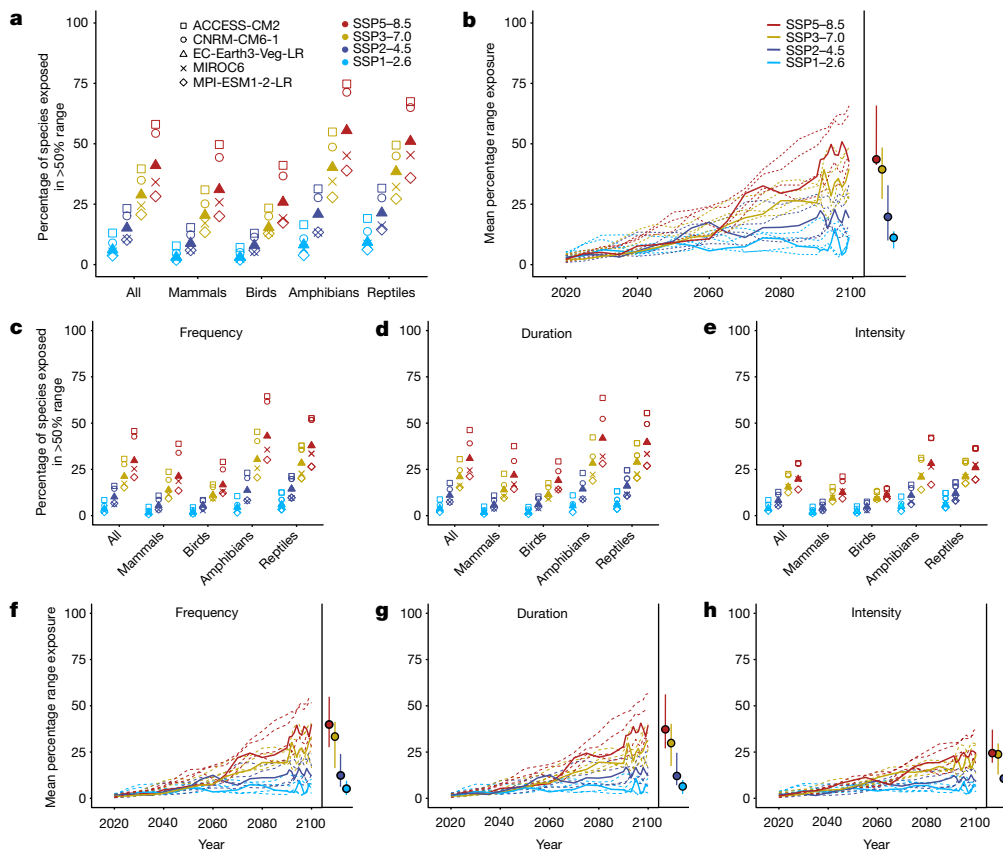


Fig. 1 | Species geographical range exposure to extreme thermal events in the future. a, c–e. The percentage of species exposed in more than half of their geographical range to extreme thermal events by 2099 for combined exposure quantified by spatially aggregating exposure to all three metrics (frequency, duration, and intensity) within the species range (a), and for each of the metric separately (frequency (c), duration (d), and intensity (e)). Actual estimates from five GCMs (different point shapes) are presented (the median model is shown as a solid triangle). **b, f–h.** The mean percentage of range exposed to extreme thermal events over time for the combined exposure to all three metrics within the species range (b), and for individual metrics (presented here for all

vertebrates combined (frequency (f), duration (g), and intensity (h)) (per-class estimates are shown in Supplementary Fig. 10). The lines are smoothed by a three-point moving average (estimates are for every five-year interval from 2015 to 2090, and every year from 2090 to 2099). Side panel represents mean percentage range exposure of the median model (circles) and range (error bar with maximum and minimum model estimates). The median model is presented as a bold line, and individual models are presented as dashed lines (b and f–h). The scenarios and the corresponding mean global warming by 2100 compared with pre-industrial conditions (1850–1900) were as follows: SSP1–2.6 (1.8 °C), SSP2–4.5 (2.7 °C), SSP3–7.0 (3.6 °C) and SSP5–8.5 (4.4 °C).

Quantifying extreme thermal events

Extreme thermal events can be defined as the period in which the temperature significantly exceeds a historical percentile threshold temperature (for example, 95th or 99th percentile) for a given duration of time^{2,34}. Species’ physiological tolerance limits are predominantly linked to extreme temperature events^{35–37}. Thus, future temperatures exceeding extreme historical temperatures will force organisms to experience conditions that they have yet to encounter, which may lower their fitness or even cause death^{7,14,19,38}. We estimated extreme thermal event characteristics on the basis of species-specific historical threshold temperatures (99th percentile of the thermal maximum (PTmax₉₉); Extended Data Fig. 1 and Methods). These thresholds were measured as the extreme temperature (top 99th percentile) that a species has experienced within their geographical range for the 1950–2005 period using daily maximum air temperature time-series data. We used PTmax₉₉ to define future extreme thermal events (see Methods and Supplementary Information for a comparison with physiological limits). We considered an extreme thermal event for a species to be a period of at least five consecutive days in which the daily maximum temperature at a site exceeds the PTmax₉₉ (details and sensitivity analyses are provided in the Methods)^{2,34}.

We quantified three metrics of extreme thermal events: (1) frequency: the number of yearly occurrences of extreme thermal events; (2) duration:

the mean number of days (between the start and end dates) of extreme thermal events in a year; and (3) intensity: the mean peak temperature (in degrees Celsius above the species-specific threshold) of all designated yearly extreme thermal events (Supplementary Fig. 1). To define the extent of species exposure to extreme thermal events, we calculated these three metrics at a grid-cell resolution of about 24.1 km² throughout each species range while comparing these three metrics between historical (1950 to 2005) and future (2015 to 2099) periods (Extended Data Fig. 1).

We provide range exposure estimates for four SSPs: SSP1–2.6 (the low-emission scenario); SSP2–4.5 (the intermediate-emission scenario); SSP3–7.0 (the intermediate-high emission scenario); and SSP5–8.5 (the high-emission scenario), from five climate models (Methods). We highlight extreme event exposure estimates for SSP5–8.5, as the recent, historical global warming trajectory most closely aligns with SSP5–8.5 (ref. 39) and to demonstrate the disastrous consequences of high, unmitigated emissions (all relevant estimates for the other scenarios are also presented). Assessments for the end of the century are averaged from estimates for each year between 2090 and 2099 (hereafter 2099). We quantify species’ range exposure in two ways: (1) as the percentage of species exposed to extreme thermal events over 50% of their geographical range by 2099 (ref. 20); and (2) the average percentage of geographical range exposed to future extreme events across all species per climate model (Methods). We calculated range

exposure measures by spatially aggregating the exposure to all three metrics (frequency, intensity, and duration) across a species' range and separately for each metric (full details are provided in the Methods).

Exposure to future extreme thermal events

Under a high greenhouse gas emission scenario (SSP5–8.5; 4.4 °C warmer world), 41.0% (median; range: 28.2–58.0%, estimates from five models) of land vertebrate species will experience extreme thermal events for all three metrics in >50% of the geographical range (Fig. 1a). Under an intermediate-high-level emission scenario (SSP3–7.0; 3.6 °C warmer world), the median estimate was 28.8% (20.7–39.6%; Fig. 1a). For SSP2–4.5 (2.7 °C warmer world)—warming similar to that expected by 2100 under current policy pledges—the median estimate was 15.1% (10.2–23.2%; Fig. 1a). Under a low-emission scenario (SSP1–2.6; 1.8 °C warmer world), the estimate is lower still (6.1% (3.7–13.0%); Fig. 1a). These results provide important quantitative evidence on how policy measures could mitigate extreme heat impacts on biodiversity¹⁷.

Across classes, the median percentage of exposure was higher for amphibians (from high to low emission: SSP5–8.5, 55.5%; SSP3–7.0, 40.2%; SSP2–4.5, 21.0%; SSP1–2.6, 8.2%) and reptiles (SSP5–8.5, 51.0%; SSP3–7.0, 38.5%; SSP2–4.5, 21.5%; SSP1–2.6, 9.3%) compared with mammals (SSP5–8.5, 31.1%; SSP3–7.0, 20.4%; SSP2–4.5, 8.8%; SSP1–2.6, 3.1%) and birds (SSP5–8.5, 25.8%; SSP3–7.0, 15.3%; SSP2–4.5, 8.0%; SSP1–2.6, 3.1%). Variation in projected exposure across taxa can be explained by differences in geographical range size⁴⁰ and the biome they occupy (Supplementary Figs. 30 and 31), and may further depend on species ecology⁴¹ (Supplementary Discussion). Exposure trends for each of the three individual metrics are lower than those based on their combination and are generally consistent across taxa (Fig. 1a,b versus Fig. 1c–h).

The mean percentage of geographical range exposure to extreme heat events for all land vertebrates will increase steadily in the coming years, most substantially for the SSP5–8.5 scenario (Fig. 1b). By the end of the twenty-first century, the mean percentage of geographical range exposure will be 45.6% (range 33.4–60.1%) for the SSP5–8.5 scenario. Notably, our estimates suggest that, under SSP5–8.5, on average 9.2% (range, 7.2–13.4%) of geographical ranges will be exposed to at least one feature of the extreme event as early as 2040 (Fig. 1b). Under the SSP1–2.6 scenario, the mean percentage range exposure will reach 8.3% (5.6–17.1%) by the end of the century (Fig. 1b). This difference between scenarios is tantamount to a delay of 60 years in extreme thermal event exposures (Fig. 1b), highlighting the considerable benefits of limiting warming to below 2 °C (ref. 20). The delay in exposure timing between scenarios is similar to previous findings for mean annual temperature²¹, suggesting a consensus among different climate change measures in terms of the gains to biodiversity in delaying exposure from emission reductions.

Assemblage-level exposure

To highlight the degree of exposure at the level of species assemblage, we calculated the percentage of species in each grid-cell exposed to the three features of extreme thermal events by 2099. We found that regions that are most exposed to extreme thermal events are in the mid-latitudes: mostly in deserts, shrublands, sub-arid regions, savanna, and grassland habitats (rather than the tropics^{9,10,19}; Fig. 2), followed by some tropical habitats (such as the Amazon basin; Extended Data Fig. 4). Specifically, most assemblages in the Mojave Desert, the Caribbean islands, the Gran Chaco, northwestern Sahara and the Sahel, Iraq, Saudi Arabia, Afghanistan, Pakistan, Botswana, eastern Namibia, northern South Africa, most of central and northwestern Australia, and many islands (such as the Caribbean and Pacific) are projected to experience a high frequency of extreme events beyond the historical limits of nearly all species under SSP5–8.5 (Fig. 2a). Some of these regions are already facing population declines due to extreme thermal events^{42–44}. Assemblages in the southern United States, most of the Amazon basin, Venezuela, the Kgalagadi

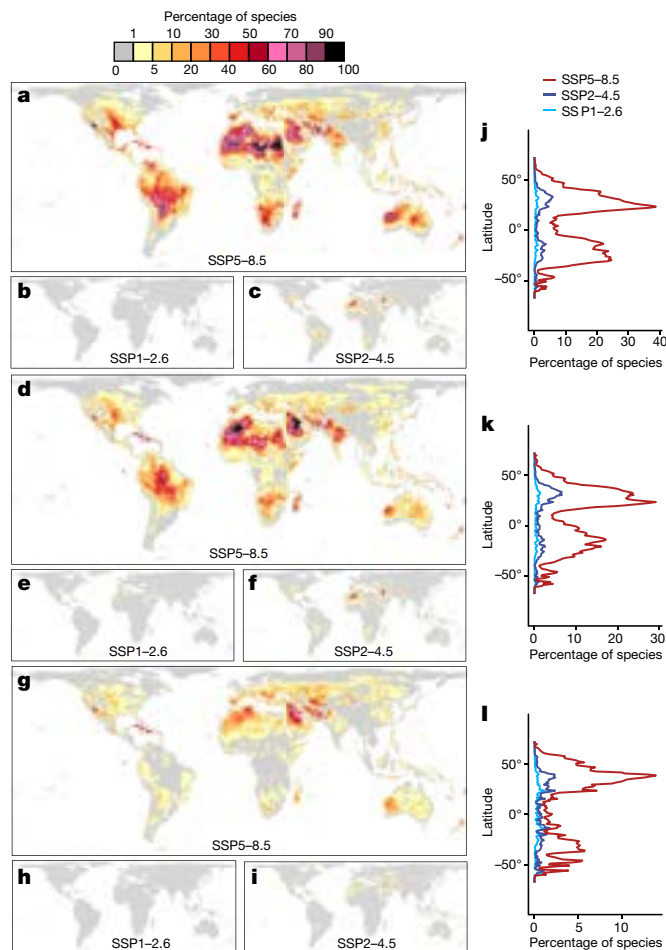


Fig. 2 | Spatial patterns of land vertebrate assemblages at risk due to extreme thermal events by 2099. Assemblage-level (that is, per grid-cell) exposure was quantified as the percentage of species present in each grid-cell exposed to the frequency (a–c), duration (d–f), and intensity (g–i) of extreme events greater than the historical levels, under the scenarios SSP5–8.5 (a, d, g), SSP1–2.6 (b, e, h) and SSP2–4.5 (c, f, i). j–l, Latitudinal patterns as the mean value per -24.1 km^2 longitudinal band are shown for the three metrics (frequency (j), duration (k), and intensity (l)). The maps show median estimates from five GCMs. See Extended Data Figs. 7–10 for the results on major taxonomic groups, and Supplementary Figs. 11–15 for the results using SSP3–7.0.

(Kalahari), western Madagascar, central India, and eastern China are at considerable exposure to frequent extreme thermal events under SSP5–8.5 (approximately 30–50% of species in an assemblage; Fig. 2a). Assemblages exposed to a high duration and intensity are mostly similar to those exposed to a high frequency of extreme events (Fig. 2a,d,g). Many assemblages in the Gran Chaco, northwestern Sahara and the Sahel, Iraq, northern South Africa, and most of central and northwestern Australia are at considerable exposure (>40%) under SSP3–7.0 (Supplementary Fig. 11). Under SSP2–4.5, only a few assemblages in Algeria, Iraq, and northwestern Australia are at greater exposure (Fig. 2c,f,i). Limiting mean global warming to below 2 °C can fully prevent species exposure to extreme thermal events in many assemblages (Fig. 2b,e,h). Under the lowest-emission scenario (SSP1–2.6), most assemblages have <1% species exposure, with greater exposure (>30% species) concentrated in islands (for example, the Caribbean and the Pacific).

Spatial patterns of exposure to extreme temperatures differ across vertebrate classes (Extended Data Figs. 7–10). Threats to island assemblages are more prominent in amphibians and reptiles compared with in mammals and birds. Generally, smaller range sizes of amphibians and reptiles are reflected in increased exposure to extreme thermal

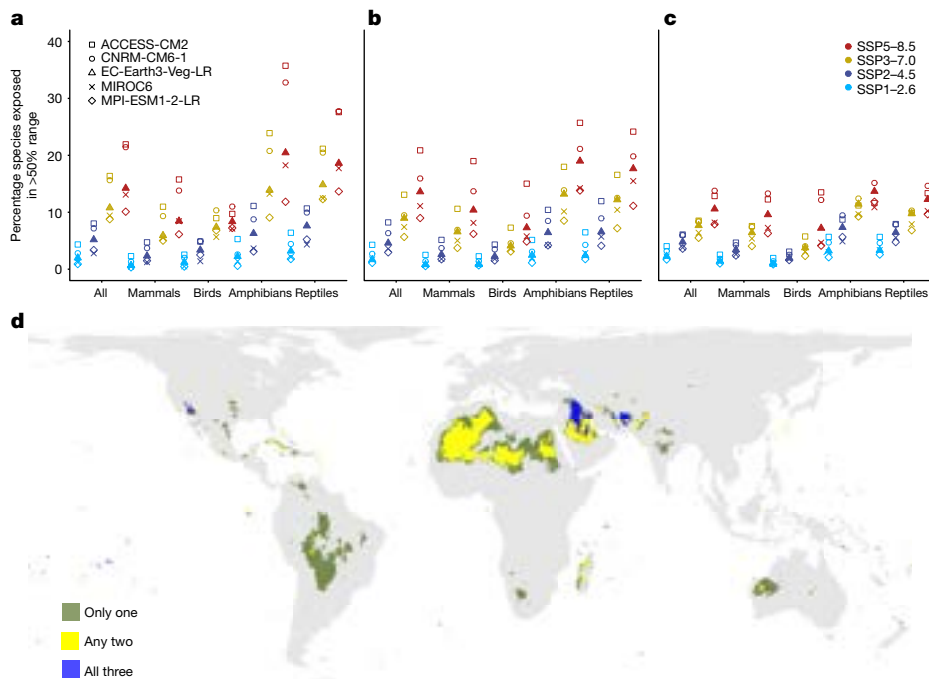


Fig. 3 | Simultaneous risk due to multiple aspects of extreme thermal events. **a–c**, Species-level exposure, calculated as the percentage of species with more than half of their geographical range to be exposed to all three metrics (frequency, duration, and intensity) (**a**), any two metrics (frequency and intensity, frequency and duration, or duration and intensity) (**b**) or a single metric (frequency, duration, or intensity) (**c**) of extreme thermal events beyond their historical levels by 2099. Actual estimates from five GCMs (different point

shapes) are presented (the median model is shown as a solid triangle). **d**, Assemblage-level exposure. Grid-cells with more than 50% of species exposed to only one, any two or all three metrics of extreme thermal events beyond their historical levels for SSP5–8.5 by 2099. Median estimates from five GCMs are shown. The results for major taxonomic groups and other SSPs are presented in Supplementary Figs. 16–18.

events by 2099—especially in Sri Lanka, Eastern Madagascar, Borneo, and Papua New Guinea—compared with mammals and birds. Endemic reptiles and bats in New Zealand also face higher exposure (Extended Data Figs. 7 and 10). The number of species projected to be exposed to extreme temperature events is positively correlated with species richness at the grid-cell level (Supplementary Figs. 21–23), suggesting that biodiverse regions, especially in the Neotropics (Supplementary Fig. 34), may also face adverse effects of extreme heat. This positive relationship is predominantly evident in amphibians and reptile species that have on average smaller ranges than birds and mammals (Spearman’s $\rho = 0.36–0.74$ in amphibians and reptiles versus $\rho = 0.03–0.51$ in mammals and birds, respectively; Supplementary Figs. 22 and 23).

We compared our results on exposure to extreme temperature events on biodiversity to the results of projected changes to mean temperatures (as explored previously^{10,21,22}). Overall, we found that assemblages in mid-latitude regions (arid regions) are more strongly exposed to extreme thermal events, whereas tropical assemblages are more exposed to changes in mean annual temperatures (Extended Data Fig. 6; see the Supplementary Discussion for explanations).

Compounded extreme exposure

The frequency, duration, and intensity of extreme events may impart different types of thermal stress to animals that are not necessarily spatially independent⁴¹. Exposure to more than one of them simultaneously probably poses a much greater risk than exposure to one separately. The percentage of species that will experience frequency, duration, and intensity of extreme events together is greater than the percentage of species that will experience a combination of any two features or only a single one (Fig. 3a–c). Under SSP5–8.5, on average 14.2% of all land vertebrates, 8.4% of mammals, 8.3% of birds, 20.4% of amphibians and 18.6% of reptiles are predicted to be exposed to all

three measures of extreme events in >50% of their range (Fig. 3a–c). The estimated median exposure to a single measure for SSP5–8.5 is 10.6% of all land vertebrates, 9.6% of mammals, 7.2% of birds, 13.7% of amphibians and 12.2% of reptiles (Fig. 3a–c). Under SSP3–7.0, the projected median exposure for all vertebrates is 10.8% for all three features, 8.9% for a combination of any two, and 7.7% for a single measure. Under the intermediate- and low-emission scenarios, there is less difference in the percentage of species that will experience either of all three features together (SSP2–4.5, 5.2%; SSP1–2.6, 2.0%, for all land vertebrates), a combination of any two (SSP2–4.5, 4.6%; SSP1–2.6, 1.7%), or a single feature (SSP2–4.5, 4.2%; SSP1–2.6, 2.3%; Fig. 3a–c).

At the assemblage level, the three types of exposure are only moderately correlated to each other, especially for the high-emission scenario (Supplementary Figs. 37 and 38). Nevertheless, under SSP5–8.5, more than 50% of vertebrate species in the southern parts of the Mojave Desert, Iraq, Afghanistan, Pakistan, and many islands in the Pacific will simultaneously face a high frequency, duration, and intensity of extreme events beyond their historical limits (Fig. 3d). Parts of the Sahara and Sahel, Saudi Arabia, and western Madagascar are projected to experience any two measures of extreme thermal events simultaneously (Fig. 3d). Most of the Amazon basin, Kgalagadi, north-western and central Australia, and central India may face only one measure of the extreme event. Notably, different vertebrate classes differ in the regions exposed to the combinations of metrics. Specifically, amphibians and reptiles in the Caribbean Islands, southwestern Europe, and eastern China are greatly exposed to the combination of exposure types compared with birds and mammals (Supplementary Fig. 18).

Living under a permanent extreme event

The mean total duration of extreme thermal events within species geographical range for all land vertebrate species in 2099 will be

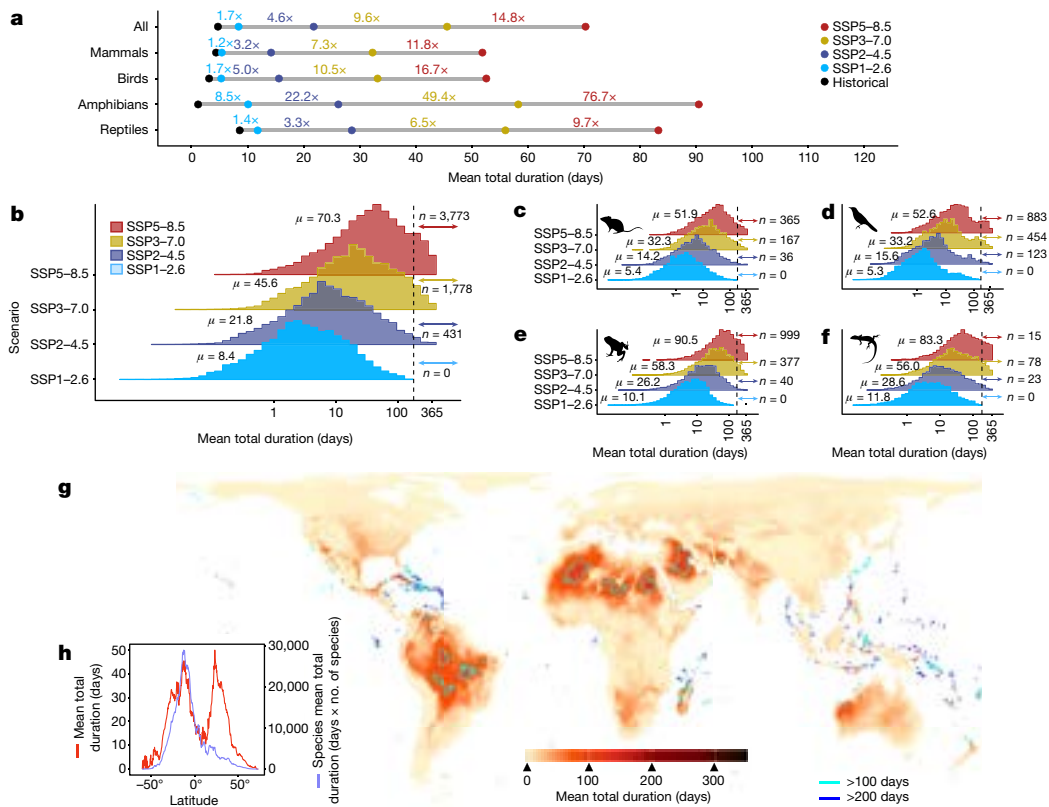


Fig. 4 | Projected total duration of exposure to extreme thermal events by 2099. **a**, The overall mean of the total duration of extreme thermal event exposure from the median model for historical and future scenarios. The values at the top of the lines represent the fold increase in the mean total duration for the future period (2099) for different SSPs compared with the historical period (1950–2005). **b–f**, The distribution of the total duration averaged within each species geographical range for all land vertebrates (**b**), mammals (**c**), birds (**d**), amphibians (**e**), and reptiles (**f**). The number of species that experience a mean total duration within their geographical range of more than 182 days per year (that is, more than half a year; vertical dashed line) is highlighted for each SSP scenario (**b–f**). The distribution’s

overall mean (μ) is represented next to the histograms for each SSP scenario. Estimates are provided as the median from five GCMs. **g**, Spatial patterns of the mean total duration per grid (that is, species assemblage) by 2099 under SSP5–8.5 (light blue borders, >100 days; dark blue borders, >200 days). **h**, Corresponding latitudinal patterns for the mean total duration of exposure per assemblage for all land vertebrates by 2099 under SSP5–8.5; the red line represents the mean total duration per 24.1 km² latitudinal band, and the violet line represents the latitudinal pattern for the mean total duration multiplied by the number of species per grid-cell. Results for other SSPs are presented in Supplementary Fig. 19.

14.8 (70.3 days, SSP5–8.5), 9.6 (45.6 days, SSP3–7.0), 4.6 (21.8 days, SSP2–4.5), and 1.8 (8.4 days, SSP1–2.6) times higher on average compared with the historical period (4.72 days; Fig 4a). Overall, 11.24% (3,773 species) of all land vertebrates are projected to face extreme thermal events totalling more than half a year (182 days) on average under SSP5–8.5 (Fig. 4b). The percentage of land vertebrates that face extreme events totalling over half a year for the projections SSP3–7.0 and SSP2–4.5 is 3.5% (1,178 species), and 1.2% (437 species), respectively. Under SSP1–2.6, no land vertebrate species will experience extreme temperature events for more than 182 days per year. Amphibians and reptiles will probably face more prolonged exposure to extreme thermal events than mammals and birds (under SSP5–8.5, mammals, 6.4%; birds, 8.7%; amphibians, 14.4%; reptiles, 14.2%; Fig. 4c–f).

Many assemblages in the mid-latitude regions (both hemispheres), including arid and sub-arid areas, and most of South America (the Amazon basin), are projected to face on average extreme thermal events of at least 100 days under SSP5–8.5 (Fig. 4g,h). However, when the mean total duration of exposure is scaled by the total number of species per assemblage, assemblages in the southern hemisphere (for example, many species-rich assemblages in the Amazon basin) will probably face higher exposure than in the northern hemisphere (Fig. 4h). Although the overall average duration of exposure in the tropics is lower, assemblages with the highest mean total duration (>200 days) are several tropical islands (including Caribbean Islands, the Malay Archipelago, and Oceania; Fig. 4g,h).

Discussion

Here we explicitly assess at the global scale the threat of future short-term extreme thermal events for 90% of land vertebrates (33,548 species). Extreme temperature events are highly detrimental to species survival^{3–7}. Our analyses of species exposure to short-term extreme thermal events consequently add much-needed conservation-relevant information beyond previous analyses that considered only the risks from changes in long-term mean climates²⁰. Future assessment of the threat from global warming should incorporate the complementary and biologically relevant measures of climate extremes^{3,8,13,28,45}. Our study further highlights those species and regions that will be most affected by the different facets of projected temperature extremes to enable pre-emptive conservation actions.

Identifying regions that are vulnerable to climate change is crucial to guide targeted conservation, but the exact locality of severe biological impact is contingent on the climatic dimension explored^{46,9,10,28,32,37}. Beyond our biologically relevant exploration of extreme temperatures, we also compared the climate-extremes results with an analysis of the potential effects of changes to mean temperatures. Mean temperatures will have the greatest impact in the tropics (Extended Data Fig. 6), as was previously shown^{10,21,46,47}. However, we find that the mid-latitudes, especially deserts, are the most exposed to threats from extreme events^{32,48} (Extended Data Fig. 6). These differences may arise from changes in the

variation of mean and extreme temperatures at daily and annual scales across the planet under climate change^{26,29} (Supplementary Fig. 33 and Supplementary Discussion).

We find that many species will experience extreme thermal events for most of the year over their geographical range by 2099 (Fig. 4). We suspect that such long exposure to heat extremes will prevent, or greatly reduce, the potential of coping strategies (such as through behaviour) to avoid extreme heat and therefore severely impact species^{33,49}. Longer and more intense heatwaves in the past decades have been reported to strongly correlate with population extirpations^{4,5}. We find that most land vertebrates exposed to extreme thermal events will be affected by more than one of the features that we explored, which can further exacerbate its effects on species persistence^{3,50}.

Range exposure to extreme events may not necessarily imply local population extinction. Nevertheless, we suspect that our assessment is a realistic approximation of species exposure to potentially dangerous temperatures, as we find that our species-specific threshold (PTmax₉₉) exceeds physiological limits for thermal tolerance measured in the laboratory, and potentially lethal or sublethal impacts of observed or simulated heatwaves for most species that we could gather data for (74.1% of 699 species in Extended Data Fig. 2, and 95.6% of 23 species in Supplementary Table 2, respectively). However, similar to previous assessments^{20,21}, our results may overestimate exposure if (1) species can shift their current range⁵¹, activity season⁵² or daily activity patterns⁵³; (2) physiological limits for thermal tolerance or operative temperatures can be different compared with realized climatic limits^{54,55}; (3) behavioural adaptations, or microhabitat use, can help species to cope with extreme temperatures^{56–58}; (4) species can evolve physiological tolerance, or show plastic responses, to extreme temperatures⁵⁹. We also suggest that the following high-level interaction factors may alter our estimates: (1) effects of species interactions⁶⁰; (2) effects of other related extreme events, such as megafires; (3) changes to precipitation regimes; (4) synergistic effects of climate and land-use changes (Supplementary Discussion). Future studies that address these limitations will be valuable in refining the overall effects of extreme temperatures on nature.

As the planet enters a new state of climate in which extreme temperatures that were once regarded rare become the norm⁶¹, it is crucial to establish conservation practices that minimize and tackle the impact of heat extremes. Approaches such as establishing or protecting microhabitats⁶², open water sources that lower the impact of short-term heat stress⁶³ or rewilding to maintain the intactness of communities after extreme events are essential^{3,62}. Importantly, we find strong effects of SSP scenarios on the impact on land vertebrates, with warming below 2 °C fully preventing exposure (above the thresholds we set) in many regions (Fig. 2). Our study therefore stresses the importance of lowering greenhouse gas emissions in reducing the impact of heat extremes on biodiversity, highlighting the urgent need for international collaborations to mitigate the magnitude of climate change⁶¹.

Online content

Any methods, additional references, Nature Portfolio reporting summaries, source data, extended data, supplementary information, acknowledgements, peer review information; details of author contributions and competing interests; and statements of data and code availability are available at <https://doi.org/10.1038/s41586-022-05606-z>.

- Fischer, E. M. & Knutti, R. Anthropogenic contribution to global occurrence of heavy-precipitation and high-temperature extremes. *Nat. Clim. Change* **5**, 560–564 (2015).
- Meehl, G. A. & Tebaldi, C. More intense, more frequent, and longer lasting heat waves in the 21st century. *Science* **305**, 994–997 (2004).
- Harris, R. M. et al. Biological responses to the press and pulse of climate trends and extreme events. *Nat. Clim. Change* **8**, 579–587 (2018).
- Till, A., Rypel, A. L., Bray, A. & Fey, S. B. Fish die-offs are concurrent with thermal extremes in north temperate lakes. *Nat. Clim. Change* **9**, 637–641 (2019).

- Smale, D. A. et al. Marine heatwaves threaten global biodiversity and the provision of ecosystem services. *Nat. Clim. Change* **9**, 306–312 (2019).
- Vasseur, D. A. et al. Increased temperature variation poses a greater risk to species than climate warming. *Proc. R. Soc. B* **281**, 20132612 (2014).
- Ma, G., Rudolf, V. H. & Ma, C. Extreme temperature events alter demographic rates, relative fitness, and community structure. *Glob. Change Biol.* **21**, 1794–1808 (2015).
- Vázquez, D. P., Gianoli, E., Morris, W. F. & Bozinovic, F. Ecological and evolutionary impacts of changing climatic variability. *Biol. Rev.* **92**, 22–42 (2017).
- Tewksbury, J. J., Huey, R. B. & Deutsch, C. A. Putting the heat on tropical animals. *Science* **320**, 1296–1297 (2008).
- Dillon, M. E., Wang, G. & Huey, R. B. Global metabolic impacts of recent climate warming. *Nature* **467**, 704–706 (2010).
- Power, S. B. & Delage, F. P. Setting and smashing extreme temperature records over the coming century. *Nat. Clim. Change* **9**, 529–534 (2019).
- Fischer, E. M., Sippel, S. & Knutti, R. Increasing probability of record-shattering climate extremes. *Nat. Clim. Change* **11**, 689–695 (2021).
- Román-Palacios, C. & Wiens, J. J. Recent responses to climate change reveal the drivers of species extinction and survival. *Proc. Natl Acad. Sci. USA* **117**, 4211–4217 (2020).
- Soroye, P., Newbold, T. & Kerr, J. Climate change contributes to widespread declines among bumble bees across continents. *Science* **367**, 685–688 (2020).
- McKechnie, A. E. & Wolf, B. O. Climate change increases the likelihood of catastrophic avian mortality events during extreme heat waves. *Biol. Lett.* **6**, 253–256 (2010).
- Maxwell, S. L. et al. Conservation implications of ecological responses to extreme weather and climate events. *Divers. Distrib.* **25**, 613–625 (2019).
- Seneviratne, S. I. et al. in *Climate Change 2021: The Physical Science Basis. Contribution of Working Group I to the Sixth Assessment Report of the Intergovernmental Panel on Climate Change* (eds Masson-Delmotte, V. et al.) Ch. 11, 1571–1759 (Cambridge Univ. Press, 2021).
- Mora, C. et al. Global risk of deadly heat. *Nat. Clim. Change* **7**, 501–506 (2017).
- Battisti, D. S. & Naylor, R. L. Historical warnings of future food insecurity with unprecedented seasonal heat. *Science* **323**, 240–244 (2009).
- Warren, R., Price, J., Graham, E., Forstnerhaeusler, N. & VanDerWal, J. The projected effect on insects, vertebrates, and plants of limiting global warming to 1.5 °C rather than 2 °C. *Science* **360**, 791–795 (2018).
- Trisos, C. H., Merow, C. & Pigot, A. L. The projected timing of abrupt ecological disruption from climate change. *Nature* **580**, 496–501 (2020).
- Deutsch, C. A. et al. Impacts of climate warming on terrestrial ectotherms across latitude. *Proc. Natl Acad. Sci. USA* **105**, 6668–6672 (2008).
- Ma, G., Hoffmann, A. A. & Ma, C.-S. Daily temperature extremes play an important role in predicting thermal effects. *J. Exp. Biol.* **218**, 2289–2296 (2015).
- Paaajmans, K. P. et al. Temperature variation makes ectotherms more sensitive to climate change. *Glob. Change Biol.* **19**, 2373–2380 (2013).
- Bütikofer, L. et al. The problem of scale in predicting biological responses to climate. *Glob. Change Biol.* **26**, 6657–6666 (2020).
- Seneviratne, S. I., Donat, M. G., Pitman, A. J., Knutti, R. & Wilby, R. L. Allowable CO₂ emissions based on regional and impact-related climate targets. *Nature* **529**, 477–483 (2016).
- Buckley, L. B. & Huey, R. B. Temperature extremes: geographic patterns, recent changes, and implications for organismal vulnerabilities. *Glob. Change Biol.* **22**, 3829–3842 (2016).
- García, R. A., Cabeza, M., Rahbek, C. & Araújo, M. B. Multiple dimensions of climate change and their implications for biodiversity. *Science* **344**, 1247579 (2014).
- Vogel, M. M. et al. Regional amplification of projected changes in extreme temperatures strongly controlled by soil moisture-temperature feedbacks. *Geophys. Res. Lett.* **44**, 1511–1519 (2017).
- Tamarin-Brodsky, T., Hodges, K., Hoskins, B. J. & Shepherd, T. G. Changes in Northern Hemisphere temperature variability shaped by regional warming patterns. *Nat. Geosci.* **13**, 414–421 (2020).
- Schär, C. et al. The role of increasing temperature variability in European summer heatwaves. *Nature* **427**, 332–336 (2004).
- Pinsky, M. L., Eikest, A. M., McCauley, D. J., Payne, J. L. & Sunday, J. M. Greater vulnerability to warming of marine versus terrestrial ectotherms. *Nature* **569**, 108–111 (2019).
- Sinervo, B. et al. Erosion of lizard diversity by climate change and altered thermal niches. *Science* **328**, 894–899 (2010).
- Perkins, S. E. & Alexander, L. V. On the measurement of heat waves. *J. Clim.* **26**, 4500–4517 (2013).
- Sunday, J. et al. Thermal tolerance patterns across latitude and elevation. *Philos. Trans. R. Soc. B* **374**, 20190036 (2019).
- Hoffmann, A. A. Physiological climatic limits in *Drosophila*: patterns and implications. *J. Exp. Biol.* **213**, 870–880 (2010).
- Buckley, L. B. & Huey, R. B. How extreme temperatures impact organisms and the evolution of their thermal tolerance. *Integr. Comp. Biol.* **56**, 98–109 (2016).
- Cohen, J. M., Fink, D. & Zuckerman, B. Avian responses to extreme weather across functional traits and temporal scales. *Glob. Change Biol.* **26**, 4240–4250 (2020).
- Schwalm, C. R., Glendon, S. & Duffy, P. B. RCP8.5 tracks cumulative CO₂ emissions. *Proc. Natl Acad. Sci. USA* **117**, 19656–19657 (2020).
- Urban, M. C. Accelerating extinction risk from climate change. *Science* **348**, 571–573 (2015).
- Jentsch, A., Kreyling, J. & Beierkuhnlein, C. A new generation of climate-change experiments: events, not trends. *Front. Ecol. Environ.* **5**, 365–374 (2007).
- Riddell, E. A. et al. Exposure to climate change drives stability or collapse of desert mammal and bird communities. *Science* **371**, 633–636 (2021).
- Welbergen, J. A., Klose, S. M., Markus, N. & Eby, P. Climate change and the effects of temperature extremes on Australian flying-foxes. *Proc. R. Soc. B* **275**, 419–425 (2008).
- McKechnie, A. E., Rushworth, I. A., Myburgh, F. & Cunningham, S. J. Mortality among birds and bats during an extreme heat event in eastern South Africa. *Austral Ecol.* **46**, 687–691 (2021).

45. Thompson, R. M., Beardall, J., Beringer, J., Grace, M. & Sardina, P. Means and extremes: building variability into community-level climate change experiments. *Ecol. Lett.* **16**, 799–806 (2013).
46. Perez, T. M., Stroud, J. T. & Feeley, K. J. Thermal trouble in the tropics. *Science* **351**, 1392–1393 (2016).
47. Huey, R. B. et al. Why tropical forest lizards are vulnerable to climate warming. *Proc. R. Soc. B* **276**, 1939–1948 (2009).
48. Kingsolver, J. G., Diamond, S. E. & Buckley, L. B. Heat stress and the fitness consequences of climate change for terrestrial ectotherms. *Funct. Ecol.* **27**, 1415–1423 (2013).
49. R. Kearney, M. Activity restriction and the mechanistic basis for extinctions under climate warming. *Ecol. Lett.* **16**, 1470–1479 (2013).
50. Rezende, E. L., Bozinovic, F., Szilágyi, A. & Santos, M. Predicting temperature mortality and selection in natural *Drosophila* populations. *Science* **369**, 1242–1245 (2020).
51. Chen, I.-C., Hill, J. K., Ohlemüller, R., Roy, D. B. & Thomas, C. D. Rapid range shifts of species associated with high levels of climate warming. *Science* **333**, 1024–1026 (2011).
52. Cohen, J. M., Lajeunesse, M. J. & Rohr, J. R. A global synthesis of animal phenological responses to climate change. *Nat. Clim. Change* **8**, 224–228 (2018).
53. Levy, O., Dayan, T., Porter, W. P. & Kronfeld-Schor, N. Time and ecological resilience: can diurnal animals compensate for climate change by shifting to nocturnal activity? *Ecol. Monogr.* **89**, e01334 (2019).
54. Faurby, S. & Araújo, M. B. Anthropogenic range contractions bias species climate change forecasts. *Nat. Clim. Change* **8**, 252–256 (2018).
55. Sunday, J. M. et al. Thermal-safety margins and the necessity of thermoregulatory behavior across latitude and elevation. *Proc. Natl Acad. Sci. USA* **111**, 5610–5615 (2014).
56. Scheffers, B. R., Edwards, D. P., Diesmos, A., Williams, S. E. & Evans, T. A. Microhabitats reduce animal's exposure to climate extremes. *Glob. Change Biol.* **20**, 495–503 (2014).
57. Huey, R. B. et al. Predicting organismal vulnerability to climate warming: roles of behaviour, physiology and adaptation. *Philos. Trans. R. Soc. B* **367**, 1665–1679 (2012).
58. Kearney, M., Shine, R. & Porter, W. P. The potential for behavioral thermoregulation to buffer “cold-blooded” animals against climate warming. *Proc. Natl Acad. Sci. USA* **106**, 3835–3840 (2009).
59. Morley, S. A., Peck, L. S., Sunday, J. M., Heiser, S. & Bates, A. E. Physiological acclimation and persistence of ectothermic species under extreme heat events. *Glob. Ecol. Biogeogr.* **28**, 1018–1037 (2019).
60. Cahill, A. E. et al. How does climate change cause extinction? *Proc. R. Soc. B* **280**, 20121890 (2013).
61. Lewis, F. et al. in *Climate Change 2021: The Physical Science Basis. Contribution of Working Group I to the Sixth Assessment Report of the Intergovernmental Panel on Climate Change* (eds Masson-Delmotte, V. et al.) 147–1926 (Cambridge Univ. Press, 2021).
62. Thakur, M. P., Bakker, E. S., Veen, G. C. & Harvey, J. A. Climate extremes, rewilding, and the role of microhabitats. *One Earth* **2**, 506–509 (2020).
63. Albright, T. P. et al. Mapping evaporative water loss in desert passerines reveals an expanding threat of lethal dehydration. *Proc. Natl Acad. Sci. USA* **114**, 2283–2288 (2017).

Publisher's note Springer Nature remains neutral with regard to jurisdictional claims in published maps and institutional affiliations.

Springer Nature or its licensor (e.g. a society or other partner) holds exclusive rights to this article under a publishing agreement with the author(s) or other rightsholder(s); author self-archiving of the accepted manuscript version of this article is solely governed by the terms of such publishing agreement and applicable law.

© The Author(s), under exclusive licence to Springer Nature Limited 2023

Daily climate data

We used daily maximum temperature as it accurately captures variation in extremes^{32,35} and is biologically appropriate for predicting acute thermal stress^{23,32}. We obtained daily maximum near-surface air temperature (tasmax) from the NASA Earth Exchange Global Daily Downscaled Projections (NEX-GDDP CMIP6) dataset⁶⁴. NEX-GDDP CMIP6 provides a bias-corrected statistically downscaled output of Coupled Model Intercomparison Project Phase 6 (CMIP6) daily temperature maximum data for historical and future climate projections for 35 General Circulation Models (GCMs) at a spatial resolution of 0.25° (~25 km at the Equator) for the period 1950 to 2100⁶⁵. We chose NEX-GDDP as this dataset's spatial and temporal resolution is better than others (such as HadEX3 or The Berkeley Earth daily climate). Moreover, NEX-GDDP CMIP6 provides modelled climatologies for 'historical' (1950–2014) and 'future' projections (2015–2100), circumventing the challenges associated with using different datasets for future and historical periods. For these reasons, NEX-GDDP daily climate data have been used in a wide range of climate change studies, especially involving extreme climates, for example, to assess the impact of extreme thermal events on agricultural crops^{66–68}, the spread of disease-causing vectors^{69–71} and changes in physical activity and sleep loss in humans^{72,73}.

We used five GCMs for our study (instead of all 35 because of computational limitations): the five GCMs were from the Australian Community Climate and Earth System Simulator, Australia (ACCESS-CM2); the Centre National de Recherches Météorologiques–Centre Européen de Recherche et de Formation Avancée en Calcul Scientifique, France (CNRM-CM6-1); the Europe wide consortium (EC-Earth3-Veg-LR); the National Institute for Environmental Studies, the University of Tokyo, Japan (MIROC6); and the Max Planck Institute for Meteorology, Germany (MPI-ESM1-2-LR). These five models were chosen to capture GCM-projected climate variability as available in the NEX-GDDP CMIP6 to represent 'cold' (MPI-ESM1-2-LR; MIROC6), 'warm' (CNRM-CM6-1; ACCESS-CM2) and 'intermediate' (EC-Earth3-Veg-LR) models quantified on the basis of the equilibrium climate sensitivity values^{74,75}. All of our impact metrics were calculated for each GCM separately and provided the median and range (minimum, maximum) of metrics across models to account for model variability whenever possible. We further compared our results using NEX-GDDP CMIP6 with the previous NEX-GDDP dataset based on the CMIP5 models (below).

Climate change scenarios

NEX-GDDP CMIP6 currently includes four plausible future climate pathways based on socioeconomic challenges for climate change mitigation in the future—SSP1–2.6, SSP2–4.5, SSP3–7.0, and SSP5–8.5⁷⁶. In SSP5–8.5, the economy is fossil-fuel driven and energy intensive⁷⁶, with mean global warming expected to reach 4.4 °C compared with the pre-industrial levels by the end of the century⁶¹. SSP5–8.5 is labelled as a high-emission scenario and is considered to be a very high baseline emission scenario (no policy baseline)⁷⁶. The SSP3–7.0 scenario includes policy shifts oriented towards national and regional issues⁷⁷, under which the mean warming may reach about 3.6 °C above pre-industrial levels by 2100⁶¹. The SSP2–4.5 scenario is a modest-emission scenario with socioeconomic trends that do not markedly differ from the historical patterns⁷⁶. Under SSP2–4.5, mean warming is expected to reach about 2.7 °C relative to the pre-industrial level by the end of the century⁶¹, which is well within reach with current policies⁷⁷. However, SSP2–4.5 still does not meet the Paris agreement goal of limiting warming between 1.5 °C to 2 °C. To align with further strong climate change mitigation policy (within reach of Paris agreement goal), we also included the low emission scenario (SSP1–2.6). Under SSP1–2.6, the mean warming is expected to be 1.8 °C (ref. ⁶¹).

Species distribution data

We used species extent of occurrence (EOO) polygons from the International Union for Conservation of Nature (IUCN)⁷⁸, BirdLife International and the Global Assessment of Reptile Distributions⁷⁹ for mammals and amphibians (IUCN, v.6.2), birds (BirdLife v.4) and reptiles (GARD v.1.7). We used only breeding, extant and native species ranges. We omitted all marine species (a list of species is provided in Supplementary Table 1). The final dataset had a total of 33,548 species representing 90.4% of currently known land vertebrate species, including 5,658 mammals, 10,074 birds, 6,932 amphibians and 10,884 reptiles.

We gridded the expert-drawn EOO polygons to equal area Behrmann grid-cells at a finer resolution than previous explorations⁸⁰ (~24.12 km × 24.12 km) using NEX-GDDP CMIP6 climate data. We opted to calculate our estimates at this relatively fine resolution to capture the local climatic variation within species ranges⁸¹. However, for species with EOOs less than the size of a grid-cell (<582 km²; especially many amphibians and reptiles) we may have under/overestimated the impact of extreme thermal events. Nevertheless, as these narrow-ranged species are the most affected by climate change^{40,82}, especially by extreme thermal events⁸³ (Supplementary Figs. 30 and 31), we did not exclude them. Furthermore, the intention of expert-verified EOO maps is to provide broad distributional information on species occurrence. EOOs are currently available for almost all land vertebrate species⁷⁹ and are therefore a better alternative to point locality data in terms of taxon coverage. However, EOOs are susceptible to commission and omission errors⁸⁰ and, as such, these limitations apply to our assessments. Our preliminary analyses (not shown) indicated that the inclusion of marginal species-distribution range (grid-cells with <10% of overlap with EOO) tends to inflate species-specific threshold estimates—for example, the duration of the extreme thermal event was >100 days for the historical period in few relatively large-ranged species that border hotter climates. Thus, for species with an overall EOO area of greater than 582 km² (one grid-cell), we considered species presence in a grid-cell only if more than 10% of the EOO polygon overlapped with the grid-cell. We performed an analysis examining the sensitivity of the results for cut-off values of 1%, 5%, 15%, and 20% (Supplementary Figs. 4–7). These results showed that estimates based on 10% overlap are tightly correlated with other cut-off values (Spearman's $\rho \approx 0.99$; Supplementary Figs. 4–7), suggesting that our results are not sensitive to the cut-off for most species.

Species-specific daily maximum temperature threshold for defining extreme thermal events

We used methods similar to studies on heatwaves for characterizing extreme thermal events^{34,84} (Supplementary Fig. 1). Owing to global warming trends^{1,2,61,85,86}, we estimated exposure for only hot (rather than cold) extreme thermal events. Heatwaves are defined as the 'prolonged duration of extremely high temperature' within a region^{34,84}. Extremely high temperatures are categorized as temperatures above a certain baseline threshold temperature—usually as the 90th or 95th percentile value of the historical temperature from the time-series data for that particular region^{84,87} or as an absolute impact-related threshold (for example, 40 °C)⁸⁸. This threshold-based approach has become very popular in studies addressing heatwaves^{2,3,5,84,85,87,89,90} as it enables the quantification of the frequency, duration, and intensity of extreme thermal events (see the next section).

We undertook a species-centred approach for estimating historical baseline threshold temperature. Species-specific threshold temperature (PTmax₉₉) was calculated as the spatial maximum of 99th percentile daily maximum air temperature for the historical period 1950 to 2005. Although NEX-GDDP CMIP6 provides climate data for the historical period until 2015, we set 1950–2005 as the baseline for ease of comparison with CMIP5 data (see the 'Spatial scale and CMIP5' section below). Importantly, we set the period 1950 to 2005 as the historical baseline instead of pre-industrial time (1850–1900) as NEX-GDDP CMIP6 historical

projections are unavailable before 1950. This makes our results conservative, as the latter part of the period already saw considerable warming. To further be conservative in our estimates of species-specific threshold temperature, we used the 99th percentile threshold instead of commonly used 90th and 95th percentile values to define extreme events^{34,84}.

The species-specific daily maximum temperature threshold was estimated in two steps (Extended Data Fig. 1). First, we estimated the 99th percentile value of the daily maximum temperature of the 55-year time-series data for each grid-cell in species geographical range. We then considered the hottest of the 99th percentile values (that is, maximum) across all of the grid-cells as PTmax₉₉. In other words, we quantified PTmax₉₉ as the 99th percentile of daily maximum temperature experienced by a species in the hottest part of its range between 1950 to 2005. We calculated PTmax₉₉ as the spatial maximum assuming that populations from the warmer edge of a species' range are closer to their upper tolerance⁹¹ and are therefore more vulnerable to extreme temperatures/climate change compared with those from cooler parts of the range^{32,92}. However, this approach underestimates exposure if populations are adapted to local climatic conditions⁹³ and for species that are active only during the daytime and warmest period of the year (Supplementary Discussion).

We used a relative instead of an absolute threshold⁸⁸ to account for differences in upper thermal tolerance limit across different species^{35,94,95}. This method has potential shortcomings associated with using EOs to estimate climatic limits^{37,96}, especially if a species range is not in equilibrium with climatic conditions, for example, due to anthropogenic impact⁵⁴, or ecological reasons such as species interactions⁹⁷. Nevertheless, our estimates of species-specific threshold limits are based on 'realized climatic limits' and provide a practical first approximation for estimating climate change impacts at the global level (and following approaches of recent studies^{21,98}). Furthermore, studies have shown associations between physiological thermal tolerance limits and the climatic extremes estimated from species ranges^{35–37,94,99,100}, suggesting that extreme events may affect the evolution of thermal tolerances and species ranges^{36,37,101} (Supplementary Discussion).

NEX-GDDP CMIP6 data for the 'historical' period are an output of GCM simulations. To validate the use of NEX-GDDP CMIP6 data for the historical period, we examined the correlation between the PTmax₉₉ estimated using the observed weather station data (ECMWF ERA5) and PTmax₉₉ values calculated using NEX-GDDP CMIP6. A strong positive correlation of thresholds estimated from the two datasets suggests that NEX-GDDP CMIP6 reflects the observed historical variation in daily maximum temperatures (Spearman's $\rho > 0.8$; Supplementary Fig. 3).

Species-specific daily maximum temperature threshold and physiological limits

We aimed to evaluate the real-world consequences of our spatial-derived species-specific thermal limits (PTmax₉₉). To this end, we compared PTmax₉₉ to physiological upper tolerance limit data at the species level measured in the laboratory under a standardized protocol³² from the GlobTherm database¹⁰². Our analysis included data for 699 land vertebrate species (211 mammals, 102 birds, 107 amphibians and 279 reptiles). We also evaluated our extreme event metrics, and species-specific threshold, by comparing them to direct biologically relevant data on the impact of extreme thermal events. We performed a literature survey about studies that have quantified population dynamics or biological impacts of extreme thermal events (heatwaves) in natural conditions or in the laboratory. In both of these analyses, our estimated PTmax₉₉ exceeds the physiological upper thermal tolerance limits measured in the laboratory and potentially lethal or sublethal impacts of observed or simulated heatwaves for most species that we could gather data for (Extended Data Fig. 2 and Supplementary Table 2). Thus, our analysis provides more-conservative estimates than those obtained in the laboratory or in a natural setting (deleterious effects of exposure to extreme climates may appear before our thresholds based on air temperatures are reached; Supplementary Discussion).

Defining extreme thermal events and their characteristics

We defined an extreme thermal event if the daily maximum temperature for a grid-cell in species range is above the species-specific PTmax₉₉ for more than five consecutive days⁸⁴. Although this five-day-window period is arbitrary, a limited set of species studied for the impact of extreme thermal events suggests that thermal events as short as a single day can have profound biological impacts (Supplementary Table 2). Thus, we consider our threshold number of days to define extreme thermal events to be biologically meaningful. Nevertheless, we repeated our analysis by using 10 or more days to define a heat event. Our estimate of species exposure to extreme thermal events for a threshold duration of >5 or >10 days is similar (Fig. 1 and Extended Data Fig. 3a,b), indicating that the choice of this value had little effect on our inference. Note that many species have not experienced extreme thermal events consecutively for more than 10 days in the historical period (Supplementary Figs. 8 and 9), again suggesting that our approach is conservative. Moreover, as we used a relative approach (see below) by comparing historical versus future metrics to quantify species range exposure, our results are likely to be less sensitive to the threshold duration.

We estimated the frequency, duration, and intensity^{34,84} (Supplementary Fig. 1) of extreme thermal events separately for all grid-cells within the species range for each calendar year for the historical period 1950 to 2005. For future estimates, we measured yearly extreme event metrics for every five years between 2015 and 2090 and for every calendar year for the end of the century (2090 to 2099). We estimated the total number of days under extreme thermal events for each grid-cell every year. Extreme thermal events that span different years (that is, lasting beyond 31 December) were treated as two separate events⁸⁹ so that the maximum total number of days for any extreme event can only be 365 or 366 days. Species in different hemispheres may experience temperature extremes at different times of the year (boreal versus austral summer). We examined the sensitivity of exposure duration for species in the southern hemisphere to a different start–end period (1 July to 30 June) to that used in the main analysis (1 January to 31 December). The estimated exposure duration within the species range was similar irrespective of the start–end period (Supplementary Discussion and Supplementary Figs. 39–41), suggesting that exposure duration is not much affected (<2% in all scenarios) by the specified start–end period.

Geographical range exposure to the extreme thermal events

Extreme thermal events have detrimental effects on species well-being based on the strength of all three metrics and their combination³ (Supplementary Table 2). However, such impact data for most species are currently unavailable. We therefore took a relative approach to quantify the effect of future extreme thermal events on species geographical range. We deemed a particular grid-cell (for each species) to be exposed to an extreme thermal event if the frequency, duration, or intensity of extreme thermal event in that grid-cell in the future is greater than the maximum value of the corresponding metric from the historical period calculated across all grid-cells (Extended Data Fig. 1). This process was repeated for each grid-cell, for each species that occupies it, and for each of the future years in our dataset (totalling 22 billion raster extract operations for all GCMs, scenarios and datasets). Furthermore, our estimates of geographical range exposure do not account for either adaptation or dispersal that may enable species to survive in extreme temperatures or expand outside their current range (Supplementary Discussion). For each species, those grid-cells (that form part of its current range) exposed to any of the three features of extreme thermal events for each year were subsequently used in the summary analysis. Exposure to the three metrics of extreme thermal events need not necessarily be correlated. To quantify overall exposure, we estimated species range exposure to the combination of extreme thermal event features by spatially aggregating the exposure measure of all three features (frequency, duration, and intensity). Spatial aggregation was

Article

performed by combining the three exposure layers to obtain overall range exposure per species as a binary map (grid-cell either exposed or not to any three features). These binary maps were then used to calculate the percentage of range exposure per species.

Spatial scale and CMIP5

In our main analysis, we used the NEX-GDDP CMIP6 dataset, which provides daily maximum data at ~ 25 km² spatial resolution. To understand how the spatial scale of the data may affect our results, we repeated our analysis using climate data as available from the CMIP6 runs at a coarse resolution⁸⁰ ($\sim 1^\circ$). In total, we used the same five GCMs similar to the NEX-GDDP CMIP6 dataset. As the CMIP6 original dataset uses different spatial grids, we regridded data to a 1° Behrmann grid-cells (96.5 km \times 96.5 km equal-area grids) using bilinear interpolation in R¹⁰³.

We also repeated all of our main analyses on exposure to extreme heat events for the previous phase of climate models (CMIP5). For this, we focused on five climate models from the NASA NEX-GDDP CMIP5 dataset (BCC-CSM1-1, CCSM4, CSIRO-Mk3-6-0, IPSL-CM5A-LR and MIROC-ESM). We chose to present the CMIP6 dataset in the main results as the updated CMIP6 dataset is better at simulating temperature extremes than its predecessor CMIP5 dataset¹⁰⁴.

Mean annual temperature

For analysis of mean annual temperature, we used daily near-surface air temperature (tas) data from the NEX-GDDP CMIP6 dataset for the same GCMs and SSP scenarios as in the main analysis on daily maximum temperature at approximately 24.12 km² resolution. We then calculated the mean annual temperature by first averaging the daily mean temperature data for each month separately and then across all the 12 months for each year from 1950 to 2099. Our analysis of exposure to changes in mean annual temperature followed procedures that were similar to those described in ref. ²¹. We first calculated the historical species-specific realized threshold limit for mean annual temperature as the spatial maximum of the mean annual temperature within the species range for the period 1950 to 2005. Then, for each year in the future (2015–2099), we identified those grid-cells within the species range in which the mean annual temperature exceeded the species-specific threshold as potentially exposed to unsuitable mean annual temperatures. Assemblage-level patterns were analysed by compiling the percentage of species in each global 24.12 km² grid-cell experiencing potentially unsuitable mean annual temperatures (Extended Data Fig. 6). For species range exposure, we calculated the percentage of the number of unsuitable grid-cells to the total number of grid-cells within the species range for each year (Extended Data Fig. 3e,f).

Reporting summary

Further information on research design is available in the Nature Portfolio Reporting Summary linked to this article.

Data availability

The NEX-GDDP CMIP6 climate data layer for the five GCMs were obtained from the NEX-GDDP CMIP6 webpage (<https://nccs.nasa.gov/services/data-collections/land-based-products/NEX-GDDP-CMIP6>; accessed January 2022). The NEX-GDDP CMIP5 climate data layer for the five GCMs were obtained from Amazon web services (<https://data.nasa.gov/Earth-Science/Amazon-Web-Services-NASA-Earth-Exchange-NEX-Globa/l/7yme-6yjr>; accessed November 2020). Climate data for the low-emission scenario were downloaded from the original CMIP6 runs (coarse resolution) from the Copernicus Climate Data Store (<https://cds.climate.copernicus.eu>; accessed January 2022). ECMFW ERA5 data were obtained from Copernicus Climate Data Store (<https://cds.climate.copernicus.eu>; accessed November 2020). Species distribution data are available for mammals and amphibians from the IUCN (<https://iucn.org>; accessed November 2020), birds from BirdLife International ([\[birdlife.org\]\(https://birdlife.org\); accessed November 2020\); reptiles from GARD initiative \(<https://doi.org/10.5061/dryad.9cnp5Hqmb>; accessed November 2020\). Physiological thermal tolerance data were obtained from the GlobTherm database \(<https://doi.org/10.1038/sdata.2018.22>; accessed November 2020\). Source data are provided with this paper.](https://</p></div><div data-bbox=)

Code availability

The R codes associated with the study are available at FigShare (<https://doi.org/10.6084/m9.figshare.16641079>).

64. Thrasher, B. et al. NASA Global daily downscaled projections, CMIP6. *Sci. Data* **9**, 262 (2022).
65. Thrasher, B., Maurer, E. P., McKellar, C. & Duffy, P. B. Bias correcting climate model simulated daily temperature extremes with quantile mapping. *Hydrol. Earth Syst. Sci.* **16**, 3309–3314 (2012).
66. Jin, Z. et al. Do maize models capture the impacts of heat and drought stresses on yield? Using algorithm ensembles to identify successful approaches. *Glob. Change Biol.* **22**, 3112–3126 (2016).
67. Zhang, L., Yang, B., Li, S., Hou, Y. & Huang, D. Potential rice exposure to heat stress along the Yangtze River in China under RCP8.5 scenario. *Agric. Forest Meteorol.* **248**, 185–196 (2018).
68. Al-Bakri, J. et al. Assessment of climate changes and their impact on barley yield in Mediterranean environment using NEX-GDDP downscaled GCMs and DSSAT. *Earth Syst. Environ.* **5**, 751–766 (2021).
69. Semakula, H. M. et al. Prediction of future malaria hotspots under climate change in sub-Saharan Africa. *Clim. Change* **143**, 415–428 (2017).
70. Iwamura, T., Guzman-Holst, A. & Murray, K. A. Accelerating invasion potential of disease vector *Aedes aegypti* under climate change. *Nat. Commun.* **11**, 2130 (2020).
71. Jones, A. E. et al. Bluetongue risk under future climates. *Nat. Clim. Change* **9**, 153–157 (2019).
72. Obradovich, N. & Fowler, J. H. Climate change may alter human physical activity patterns. *Nat. Hum. Behav.* **1**, 0097 (2017).
73. Obradovich, N., Migliorini, R., Mednick, S. C. & Fowler, J. H. Nighttime temperature and human sleep loss in a changing climate. *Sci. Adv.* **3**, e1601555 (2017).
74. Meehl, G. A. et al. Context for interpreting equilibrium climate sensitivity and transient climate response from the CMIP6 Earth system models. *Sci. Adv.* **6**, eaba1981 (2020).
75. Hausfather, Z., Marvel, K., Schmidt, G. A., Nielsen-Gammon, J. W. & Zelinka, M. Climate simulations: recognize the ‘hot model’ problem. *Nature* **605**, 26–29 (2022).
76. O’Neill, B. C. et al. The scenario model intercomparison project (ScenarioMIP) for CMIP6. *Geosci. Model Dev.* **9**, 3461–3482 (2016).
77. IPCC Special Report on Global Warming of 1.5°C (eds Masson-Delmotte, V. et al.) (WMO, 2018).
78. *IUCN Red List of Threatened Species Version 2017*, 3 (IUCN, 2017).
79. Roll, U. et al. The global distribution of tetrapods reveals a need for targeted reptile conservation. *Nat. Ecol. Evol.* **1**, 1677 (2017).
80. Hurlbert, A. H. & Jetz, W. Species richness, hotspots, and the scale dependence of range maps in ecology and conservation. *Proc. Natl Acad. Sci. USA* **104**, 13384–13389 (2007).
81. Maclean, I. M. Predicting future climate at high spatial and temporal resolution. *Glob. Change Biol.* **26**, 1003–1011 (2020).
82. Warren, R. et al. Quantifying the benefit of early climate change mitigation in avoiding biodiversity loss. *Nat. Clim. Change* **3**, 678–682 (2013).
83. Jiguet, F. et al. Thermal range predicts bird population resilience to extreme high temperatures. *Ecol. Lett.* **9**, 1321–1330 (2006).
84. Hobday, A. J. et al. A hierarchical approach to defining marine heatwaves. *Prog. Oceanogr.* **141**, 227–238 (2016).
85. Laufkötter, C., Zscheischler, J. & Frölicher, T. L. High-impact marine heatwaves attributable to human-induced global warming. *Science* **369**, 1621–1625 (2020).
86. Coumou, D. & Rahmstorf, S. A decade of weather extremes. *Nat. Clim. Change* **2**, 491–496 (2012).
87. Oliver, E. C. et al. Longer and more frequent marine heatwaves over the past century. *Nat. Commun.* **9**, 1324 (2018).
88. Field, C. B., Barros, V., Stocker, T. F. & Dahe, Q. *Managing the Risks of Extreme Events and Disasters to Advance Climate Change Adaptation: Special Report of the Intergovernmental Panel on Climate Change* (Cambridge Univ. Press, 2012).
89. Woolway, R. I. et al. Lake heatwaves under climate change. *Nature* **589**, 402–407 (2021).
90. Gruber, N., Boyd, P. W., Frölicher, T. L. & Vogt, M. Biogeochemical extremes and compound events in the ocean. *Nature* **600**, 395–407 (2021).
91. Cahill, A. E. et al. Causes of warm-edge range limits: systematic review, proximate factors and implications for climate change. *J. Biogeogr.* **41**, 429–442 (2014).
92. Wiens, J. J. Climate-related local extinctions are already widespread among plant and animal species. *PLoS Biol.* **14**, e2001104 (2016).
93. Valladares, F. et al. The effects of phenotypic plasticity and local adaptation on forecasts of species range shifts under climate change. *Ecol. Lett.* **17**, 1351–1364 (2014).
94. Bennett, J. M. et al. The evolution of critical thermal limits of life on Earth. *Nat. Commun.* **12**, 1198 (2021).
95. Sunday, J. M., Bates, A. E. & Dulvy, N. K. Thermal tolerance and the global redistribution of animals. *Nat. Clim. Change* **2**, 686–690 (2012).
96. Pearson, R. G. & Dawson, T. P. Predicting the impacts of climate change on the distribution of species: are bioclimate envelope models useful? *Glob. Ecol. Biogeogr.* **12**, 361–371 (2003).

97. Louthan, A. M., Doak, D. F. & Angert, A. L. Where and when do species interactions set range limits? *Trends Ecol. Evol.* **30**, 780–792 (2015).
98. Barbarossa, V. et al. Threats of global warming to the world's freshwater fishes. *Nat. Commun.* **12**, 1701 (2021).
99. Clusella-Trullas, S., Blackburn, T. M. & Chown, S. L. Climatic predictors of temperature performance curve parameters in ectotherms imply complex responses to climate change. *Am. Nat.* **177**, 738–751 (2011).
100. Qu, Y.-F. & Wiens, J. J. Higher temperatures lower rates of physiological and niche evolution. *Proc. R. Soc. B* **287**, 20200823 (2020).
101. Pither, J. Climate tolerance and interspecific variation in geographic range size. *Proc. R. Soc. Lond. B* **270**, 475–481 (2003).
102. Bennett, J. M. et al. GlobTherm, a global database on thermal tolerances for aquatic and terrestrial organisms. *Sci. Data* **5**, 180022 (2018).
103. R Core Team R: *A Language and Environment for Statistical Computing* (R Foundation for Statistical Computing, 2019); <http://www.R-project.org/>
104. Chen, H., Sun, J., Lin, W. & Xu, H. Comparison of CMIP6 and CMIP5 models in simulating climate extremes. *Sci. Bull.* **65**, 1415–1418 (2020).

Acknowledgements We thank the staff at the IUCN for making the species distribution data publicly available; J. Rosenblatt for allowing us to use his server. U.R. and S.M. acknowledge funding from the Israeli Science Foundation (grant no. ISF-406/19); G.M. is supported by the Swiss Institute for Dryland Environmental and Energy Research, and the Planning and

Budgeting Committee postdoctoral fellowships. Climate scenarios used were from the NEX-GDDP CMIP6 dataset, prepared by the Climate Analytics Group and NASA Ames Research Center using the NASA Earth Exchange, and distributed by the NASA Center for Climate Simulation (NCCS). We acknowledge the computational resources provided by the High-Performance Computation facility at the Ben-Gurion University of the Negev (BGU HPC) and the Ben-Gurion University of the Negev Department of Computer Science clusters (BGU ISE-CS-DT).

Author contributions G.M. conceived the study, developed the methods, handled all data processing, performed the analyses and generated the figures with input from T.I., S.M. and U.R. All of the authors contributed to writing of the manuscript.

Competing interests The authors declare no competing interests.

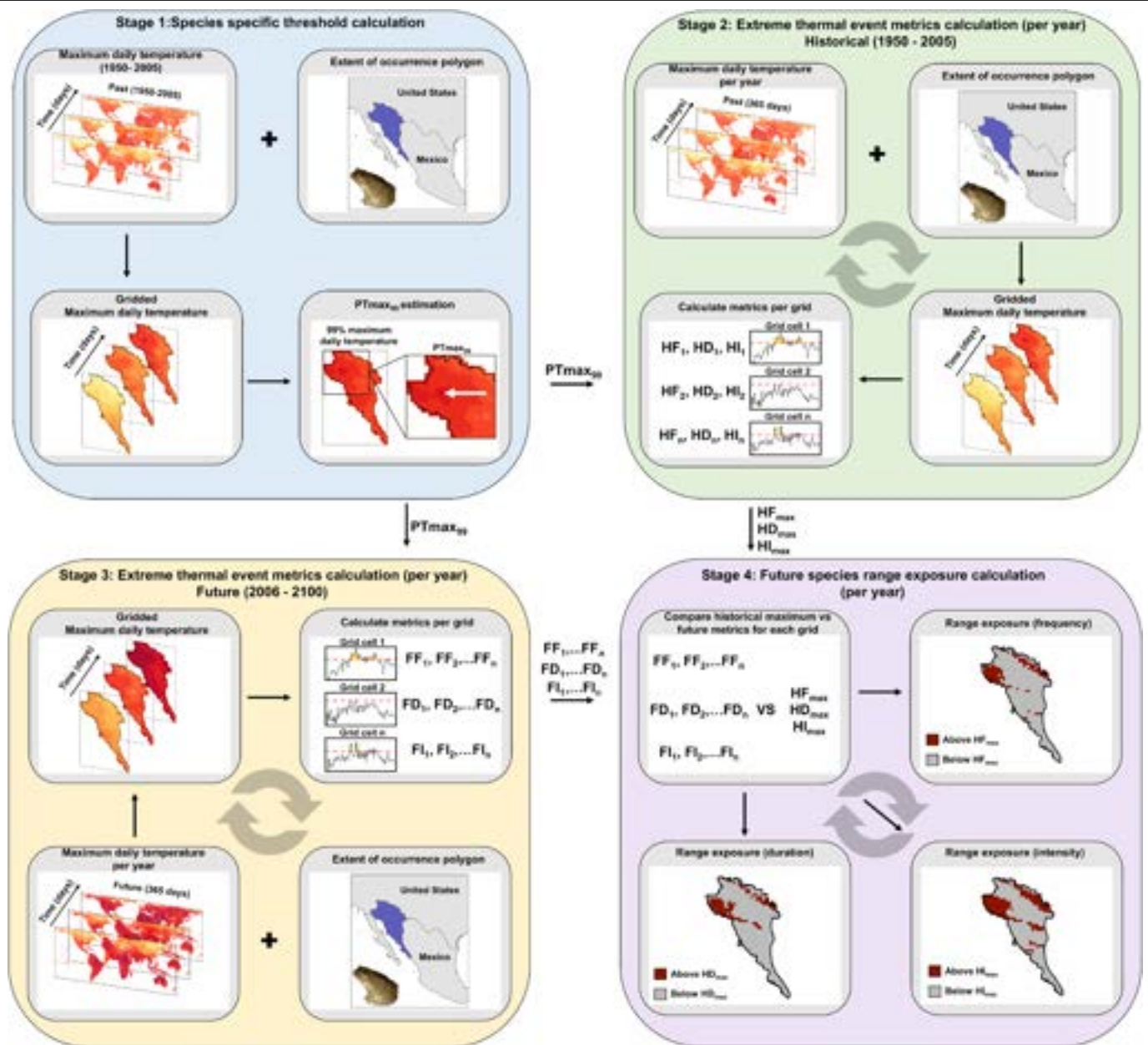
Additional information

Supplementary information The online version contains supplementary material available at <https://doi.org/10.1038/s41586-022-05606-z>.

Correspondence and requests for materials should be addressed to Gopal Murali.

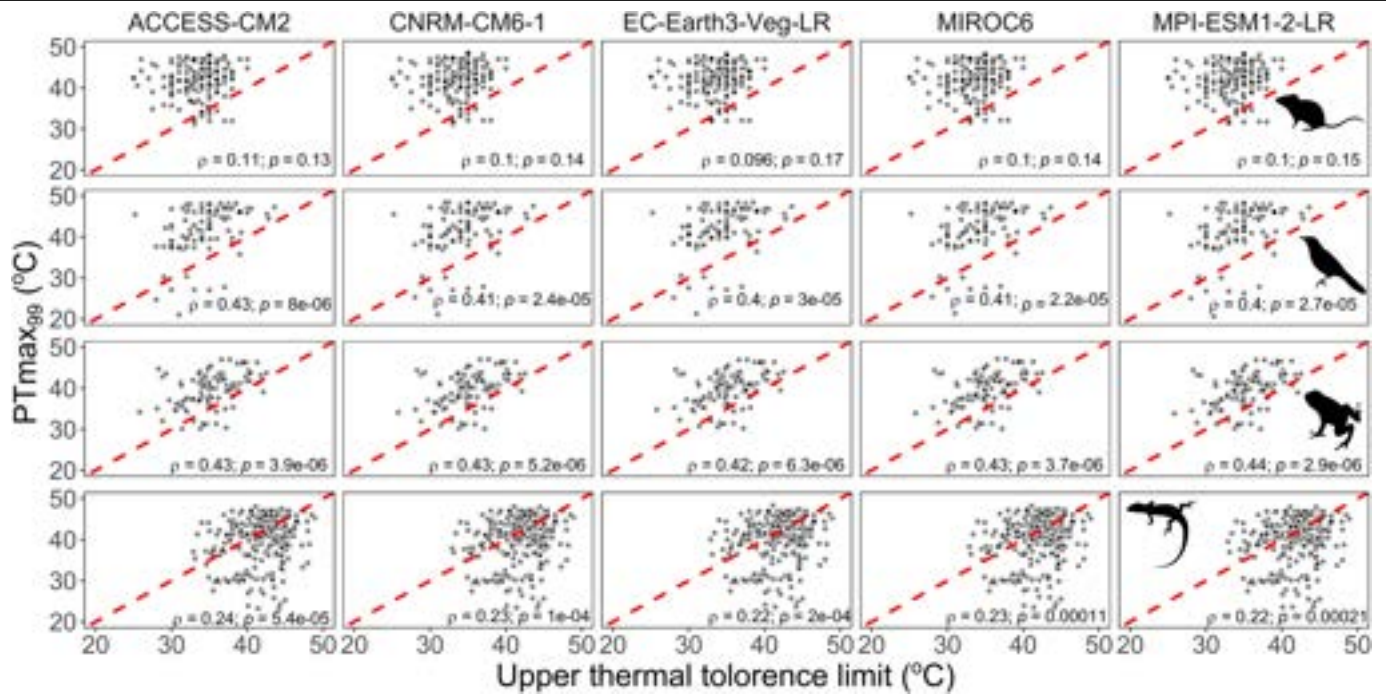
Peer review information *Nature* thanks Raymond Huey, Alex Pigot and the other, anonymous, reviewer(s) for their contribution to the peer review of this work. Peer reviewer reports are available.

Reprints and permissions information is available at <http://www.nature.com/reprints>.



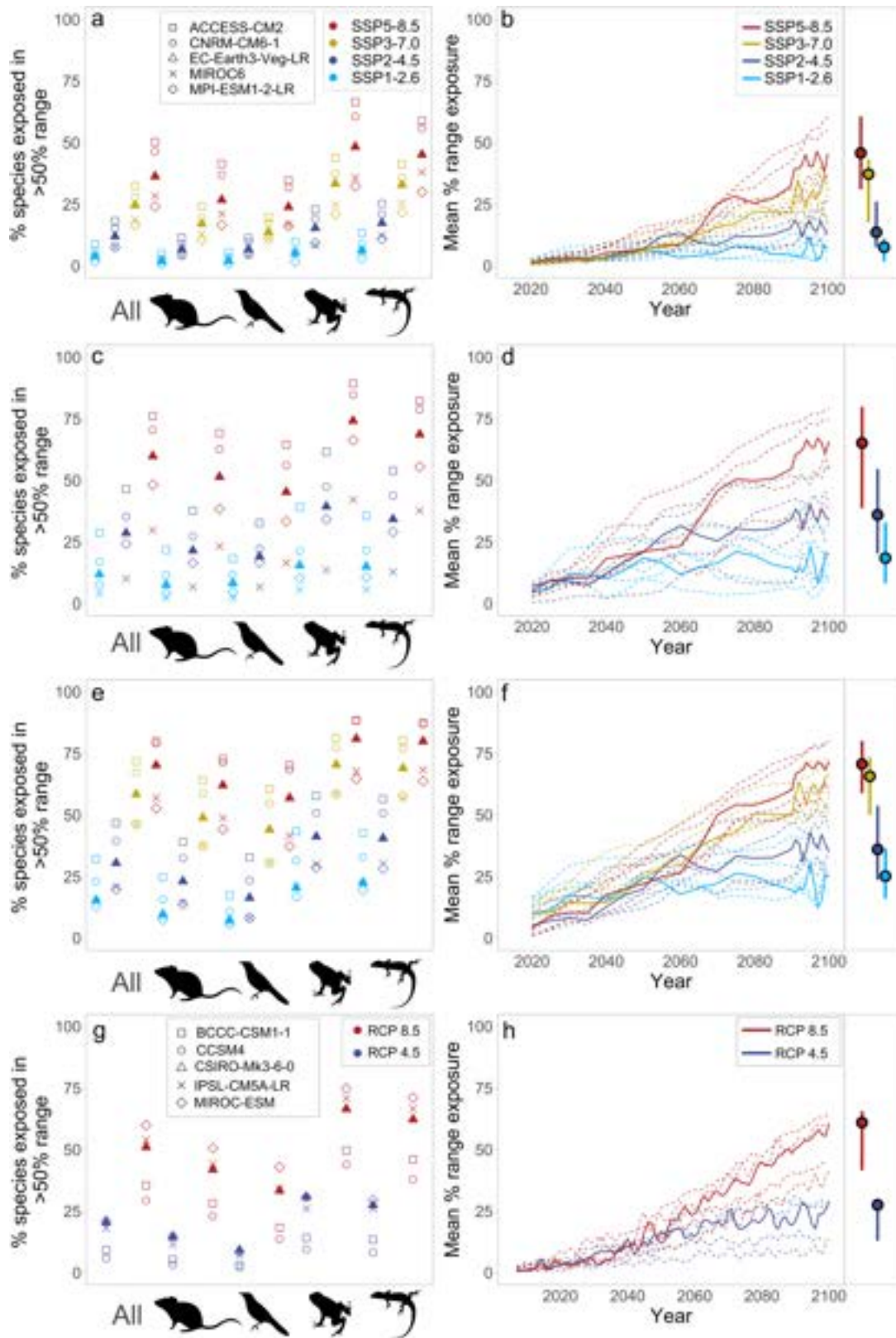
Extended Data Fig. 1 | Overview of methods employed for estimating species range exposure to extreme thermal events. Illustrated using the geographical range of the Colorado river toad *Inciilius alvarius*. **Stage 1:** species-specific threshold is calculated as the spatial maximum of 99% daily maximum temperature between the years 1950 to 2005 (PTmax₉₉ - indicated by a red arrow). **Stage 2 and 3:** extreme thermal event metrics - frequency (F), duration (D), and intensity (I) for future (indicated by letter F before each metric) and historical (indicated by letter H before each metric) period was calculated

by comparing PTmax₉₉ with daily maximum temperature time series per grid-cell for each year. Extreme event was designated if the daily maximum temperature is above the species-specific threshold for more than 5 or 10 consecutive days. **Stage 4:** to designate grid-cell exposure, future extreme event metric per year was compared against the maximum of historical metric (HF_{max}, HD_{max}, and HI_{max}). Stage 2 to 4 are repeated for each year (indicated by the circular arrow).



Extended Data Fig. 2 | Comparisons of species-specific thresholds ($PT_{max_{99}}$) and physiological upper thermal tolerances. Species physiological upper thermal tolerance data [the upper boundary of the thermal neutral zone (UTNZ) for mammals and birds; critical thermal maximum (CT_{max}) for reptiles and

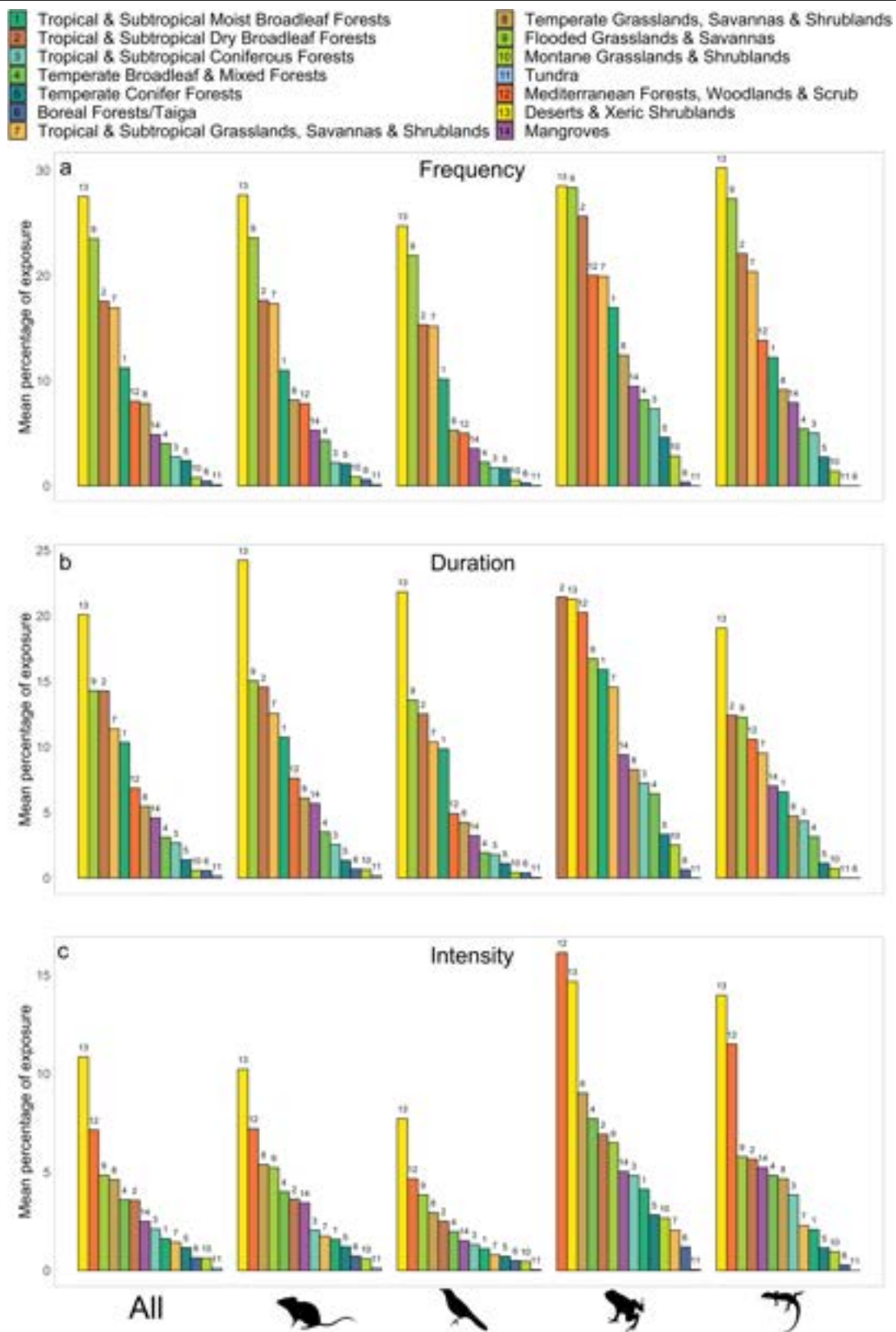
amphibians] are compared against the model specific species-specific threshold ($PT_{max_{99}}$) estimated from the NEX-GDDP CMIP6 dataset for each taxonomic group. Two-sided unadjusted P-values and ρ – Spearman's correlation coefficient are shown. 1:1 line represented with red dashed line.



Extended Data Fig. 3 | See next page for caption.

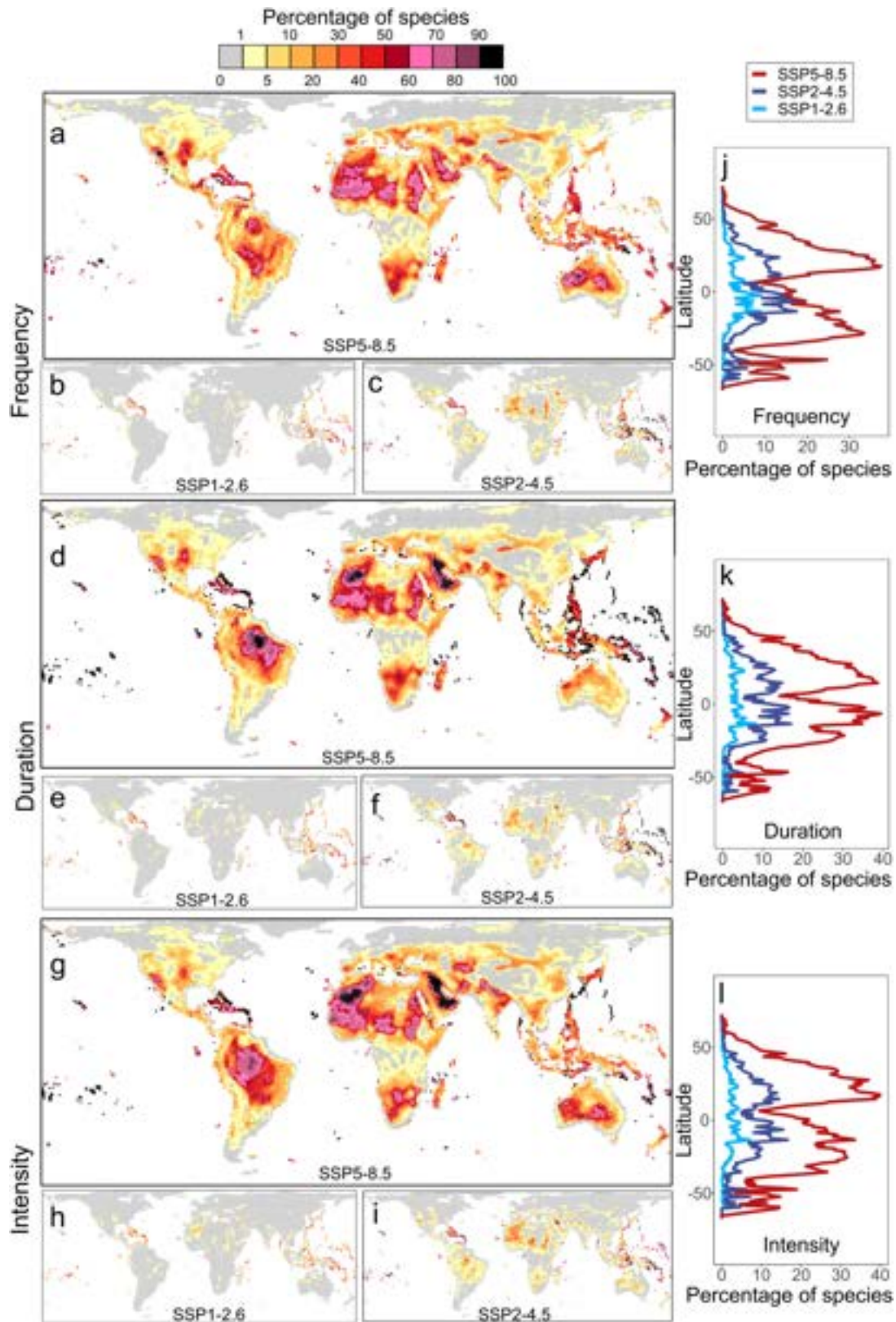
Extended Data Fig. 3 | Species geographical range exposure under different thresholds and datasets. Results presented for **a–b** when the minimal number of days required to define extreme thermal events was more than 10 days instead of 5 days (uses NEX-GDDP CMIP6 dataset), **c–d** for three different SSPs using a coarse resolution dataset ($\sim 6.5 \text{ km}^2$ grid-cells; CMIP6 original runs), **e–f** estimates based on mean annual temperature (NEP-GDDP CMIP6), and **g–h** for data from NEX-GDDP CMIP5 dataset. (**a, c, and g**) percentage of species exposed in more than half of their geographical range to extreme thermal events by 2099 for combined exposure quantified by spatially aggregating exposure to all three metrics within the species range. Actual estimates from five GCMs

(different point shapes) are presented (median model as solid triangle). (**b, d, and h**) mean percentage of range exposed to extreme thermal events over time as the combined exposure to all three metrics across species range. Side panel represents mean percentage range exposure of the median model (circles) and range (error bar with maximum and minimum model estimates). Estimate from five GCMs are presented per SSP scenario (the median model is highlighted as solid line). **e–f** same as in the other panel but uses mean annual temperature data (see methods). Scenarios and corresponding mean global warming by 2100 compared to pre-industrial conditions (1850–1900): SSP1–2.6 (1.8 °C), SSP2–4.5 (2.7 °C), SSP3–7.0 (3.6 °C), and SSP5–8.5 (4.4 °C).



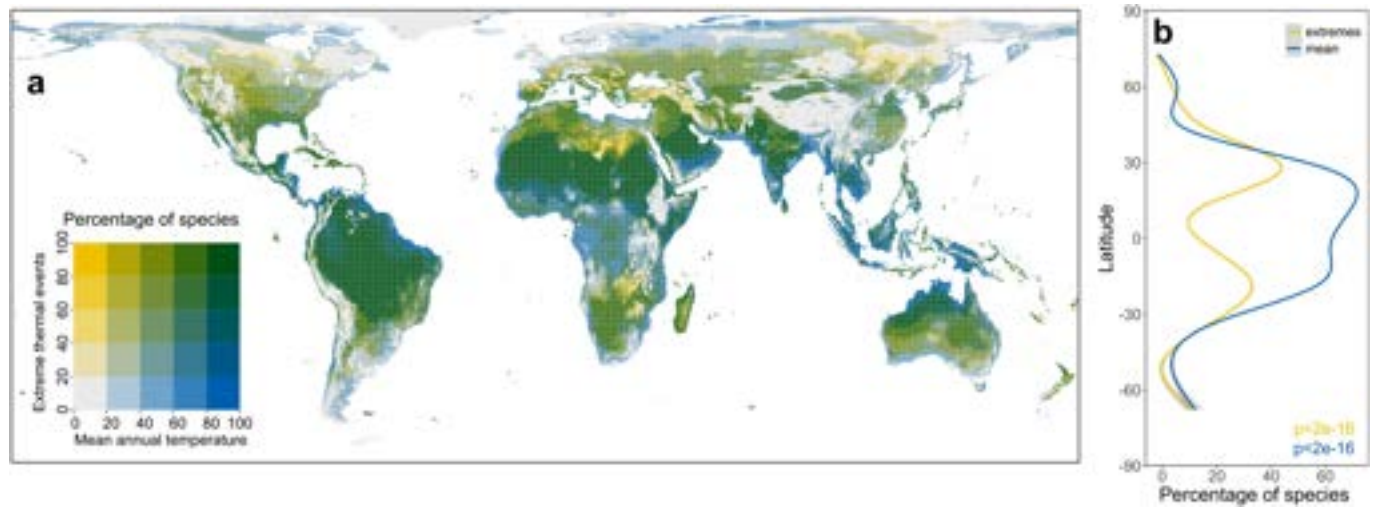
Extended Data Fig. 4 | Percentage of species exposed to extreme thermal events per assemblage averaged across 14 biome types by 2099. Results are shown for **a.** frequency, **b.** duration, and **c.** intensity of extreme events for all land vertebrates and major taxonomic groups. The numbers on top of the bar plot

represent the corresponding biome type (legend provided on top of the figure). Results are shown for the SSP5–8.5. Results for other scenarios are presented in Supplementary Fig. S27–S29. SSP5–8.5 corresponds to a mean global warming of 4.4 °C by 2100 compared to pre-industrial conditions (1850–1900).



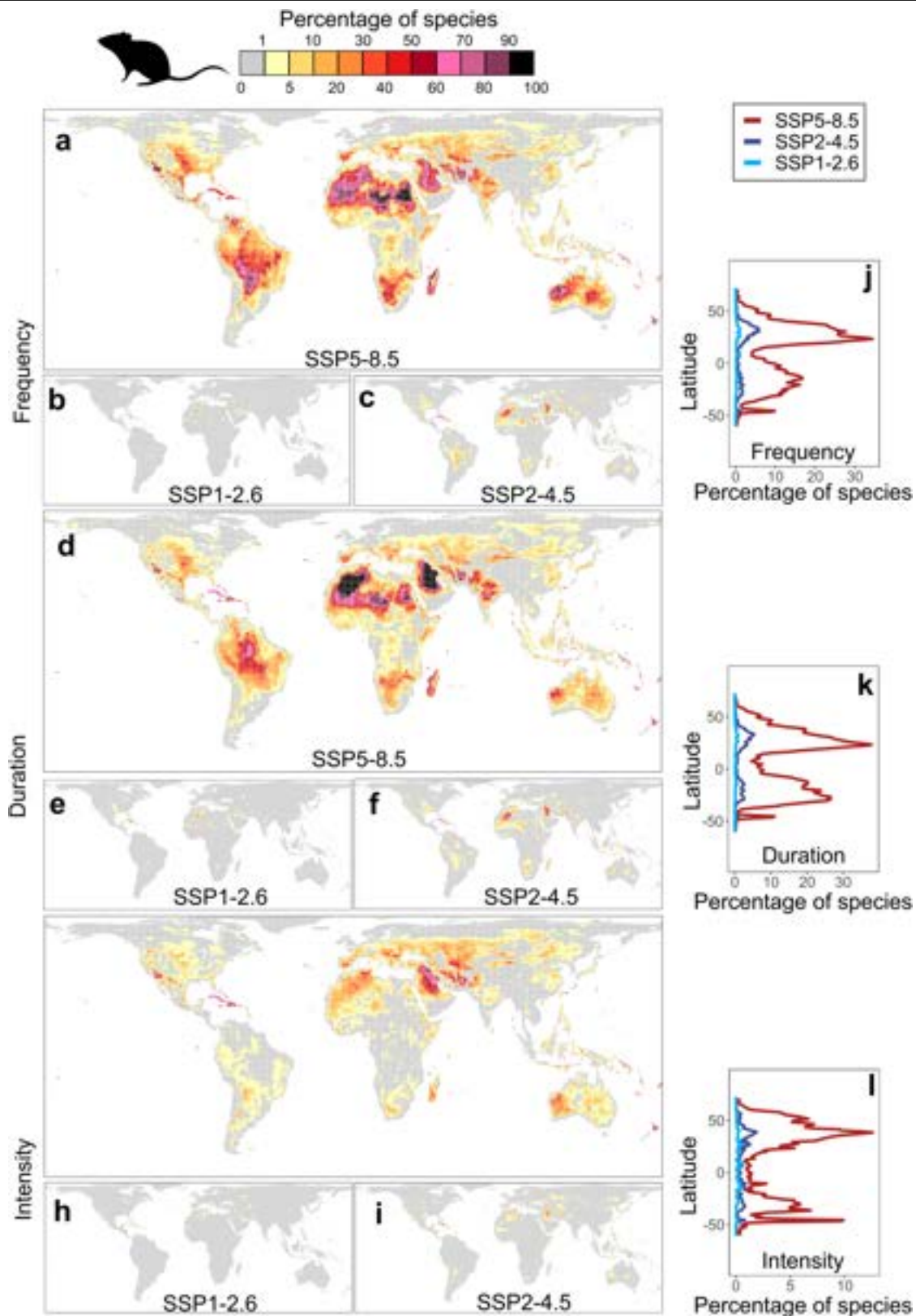
Extended Data Fig. 5 | Spatial patterns of vertebrate assemblages at risk due to extreme thermal events by 2099 for data using coarse resolution (~96.5 km² grid-cell) climate data. Assemblage level (i.e., per grid-cell) exposure was quantified as the percentage of species present in each grid-cell exposed to **a–c** frequency, **d–f** duration, and **g–i** intensity of extreme events

beyond their historical levels (corresponding latitudinal patterns as mean value per 96.5 km² grid latitudinal band is presented in **j–l**). Median estimates from five GCMs are shown. Scenarios and corresponding mean global warming by 2100 compared to pre-industrial conditions (1850–1900): SSP1-2.6 (1.8 °C), SSP2-4.5 (2.7 °C), SSP3-7.0 (3.6 °C), and SSP5-8.5 (4.4 °C).



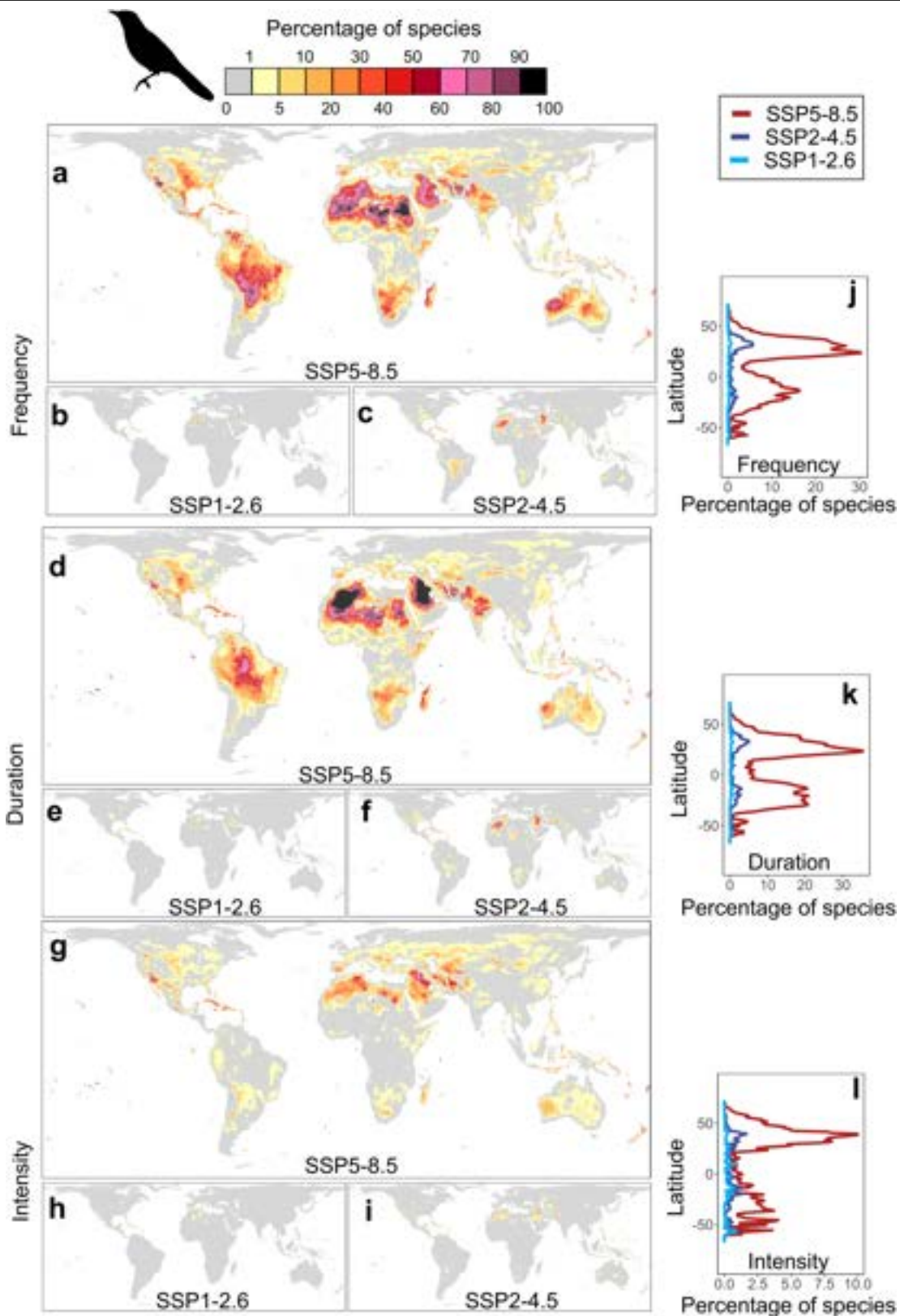
Extended Data Fig. 6 | Regionally contrasting tropical species vulnerability to mean and extreme temperatures by 2099. Bivariate map showing assemblage level percentage of vertebrate species exposure to extreme thermal events and mean annual temperature (a). For extreme thermal events, combined exposure was quantified by spatially aggregating exposure to all three metrics across the species range (same as in Fig. 1b), percentage of species exposure was then aggregated within each ~ 24.1 km² grid-cells.

b latitudinal patterns for assemblage level exposure to extreme thermal events (yellow) and mean annual temperatures (blue) are shown. Smoothened line represents generalized additive model fits of the percentage of species exposure against the latitude value of each grid-cell (GAM; both two-sided unadjusted $P < 0.001$). Median estimates from five GCMs are shown. Results are presented for the SSP5-8.5 scenario - 4.4 °C of warming by 2099 compared to pre-industrial conditions (1850-1900).



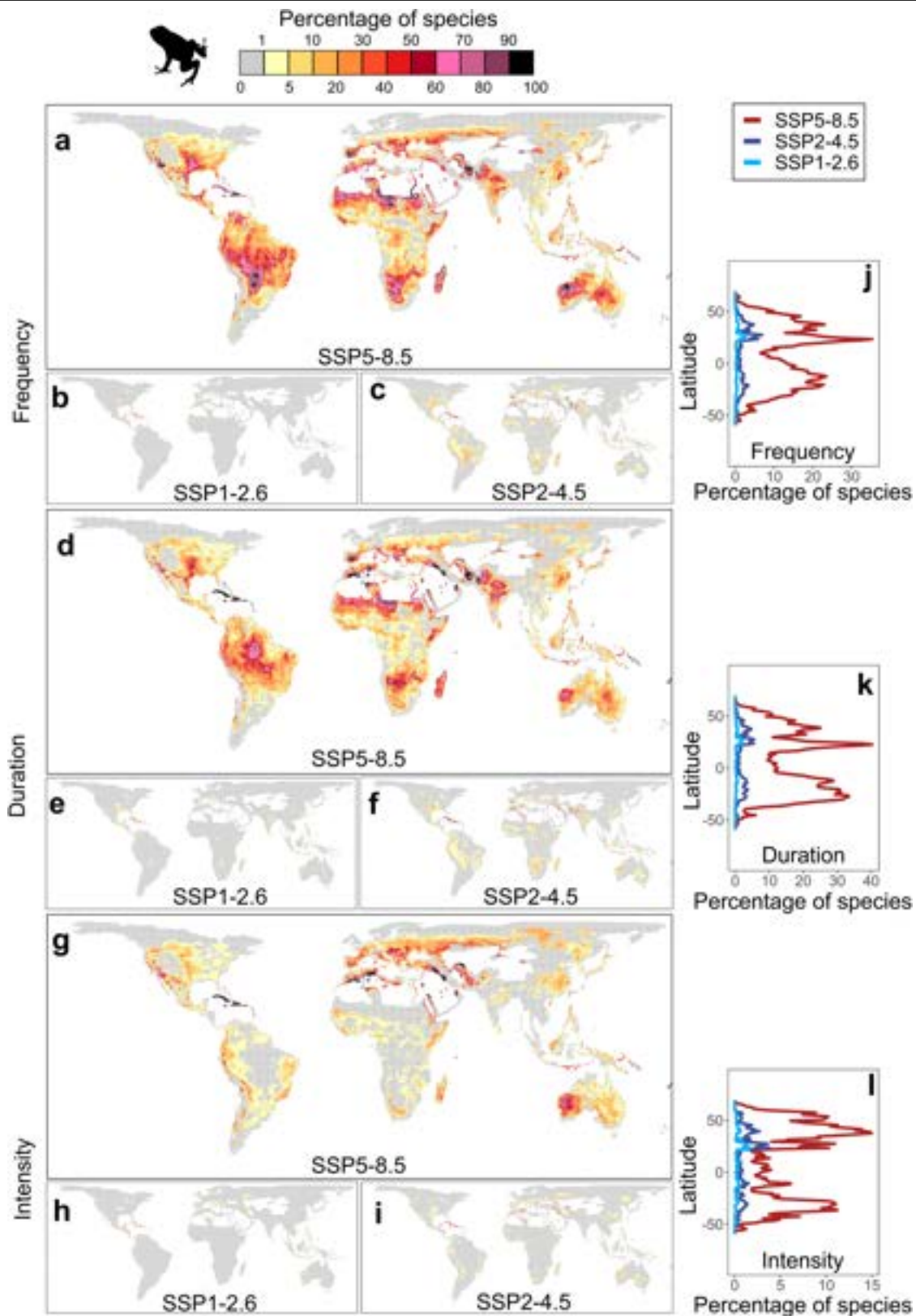
Extended Data Fig. 7 | Spatial patterns of mammal assemblages at risk due to extreme thermal events by 2099. Assemblage level (i.e., per grid-cell) exposure was quantified as the percentage of species present in each grid-cell exposed to **a–c** frequency, **d–f** duration, and **g–i** intensity of extreme events greater than the historical levels. Latitudinal patterns as the mean value per -24.1 km^2 latitudinal

band are shown in **j–l**. See Supplementary Fig. S12 to S15 for results using SSP3–7.0. Maps show median estimates from five GCMs. Scenarios and corresponding mean global warming by 2100 compared to pre-industrial conditions (1850–1900): SSP1–2.6 (1.8 °C), SSP2–4.5 (2.7 °C), SSP3–7.0 (3.6 °C), and SSP5–8.5 (4.4 °C).



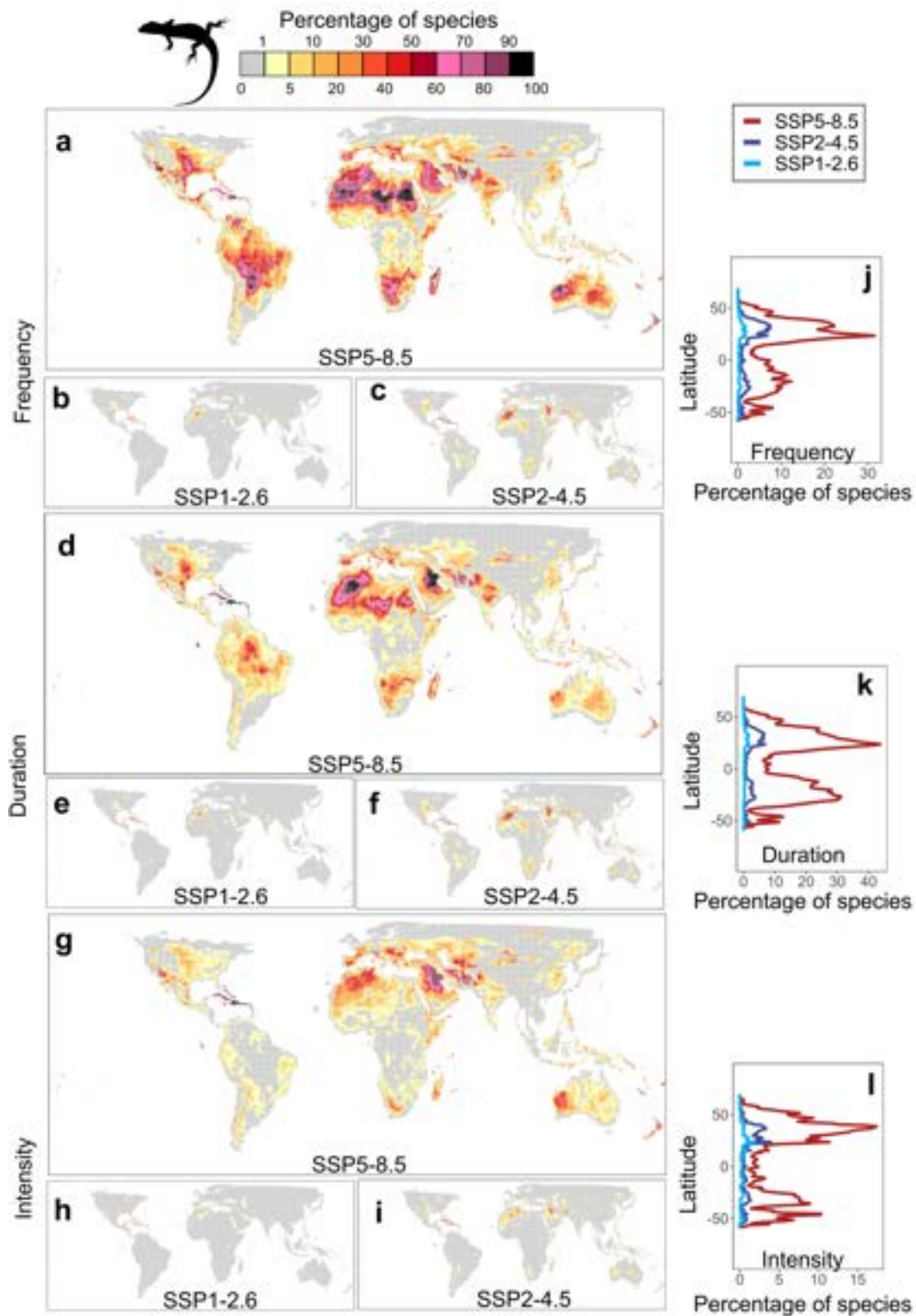
Extended Data Fig. 8 | Spatial patterns of bird assemblages at risk due to extreme thermal events by 2099. Assemblage level (i.e., per grid-cell) exposure was quantified as the percentage of species present in each grid-cell exposed to **a–c** frequency, **d–f** duration, and **g–i** intensity of extreme events greater than the historical levels. Latitudinal patterns as the mean value per -24.1 km^2 latitudinal

band are shown in **j–l**. See Supplementary Fig. S12 to S15 for results using SSP3–7.0. Maps show median estimates from five GCMs. Scenarios and corresponding mean global warming by 2100 compared to pre-industrial conditions (1850–1900): SSP1–2.6 (1.8 °C), SSP2–4.5 (2.7 °C), SSP3–7.0 (3.6 °C), and SSP5–8.5 (4.4 °C).



Extended Data Fig. 9 | Spatial patterns of amphibian assemblages at risk due to extreme thermal events by 2099. Assemblage level (i.e., per grid-cell) exposure was quantified as the percentage of species present in each grid-cell exposed to **a–c** frequency, **d–f** duration, and **g–i** intensity of extreme events greater than the historical levels. Latitudinal patterns as the mean value per

-24.1 km^2 latitudinal band are shown in **j–l**. See Supplementary Fig. S12 to S15 for results using SSP3–7.0. Maps show median estimates from five GCMs. Scenarios and corresponding mean global warming by 2100 compared to pre-industrial conditions (1850–1900): SSP1–2.6 (1.8 °C), SSP2–4.5 (2.7 °C), SSP3–7.0 (3.6 °C), and SSP5–8.5 (4.4 °C).



Extended Data Fig. 10 | Spatial patterns of reptilian assemblages at risk due to extreme thermal events by 2099. Assemblage level (i.e., per grid-cell) exposure was quantified as the percentage of species present in each grid-cell exposed to **a–c** frequency, **d–f** duration, and **g–i** intensity of extreme events greater than the historical levels. Latitudinal patterns as the mean value per -24.1 km^2 latitudinal

band are shown in **j–l**. See Supplementary Fig. S12 to S15 for results using SSP3–7.0. Maps show median estimates from five GCMs. Scenarios and corresponding mean global warming by 2100 compared to pre-industrial conditions (1850–1900): SSP1–2.6 (1.8 °C), SSP2–4.5 (2.7 °C), SSP3–7.0 (3.6 °C), and SSP5–8.5 (4.4 °C).

Reporting Summary

Nature Portfolio wishes to improve the reproducibility of the work that we publish. This form provides structure for consistency and transparency in reporting. For further information on Nature Portfolio policies, see our [Editorial Policies](#) and the [Editorial Policy Checklist](#).

Statistics

For all statistical analyses, confirm that the following items are present in the figure legend, table legend, main text, or Methods section.

n/a Confirmed

- The exact sample size (n) for each experimental group/condition, given as a discrete number and unit of measurement
- A statement on whether measurements were taken from distinct samples or whether the same sample was measured repeatedly
- The statistical test(s) used AND whether they are one- or two-sided
Only common tests should be described solely by name; describe more complex techniques in the Methods section.
- A description of all covariates tested
- A description of any assumptions or corrections, such as tests of normality and adjustment for multiple comparisons
- A full description of the statistical parameters including central tendency (e.g. means) or other basic estimates (e.g. regression coefficient) AND variation (e.g. standard deviation) or associated estimates of uncertainty (e.g. confidence intervals)
- For null hypothesis testing, the test statistic (e.g. F , t , r) with confidence intervals, effect sizes, degrees of freedom and P value noted
Give P values as exact values whenever suitable.
- For Bayesian analysis, information on the choice of priors and Markov chain Monte Carlo settings
- For hierarchical and complex designs, identification of the appropriate level for tests and full reporting of outcomes
- Estimates of effect sizes (e.g. Cohen's d , Pearson's r), indicating how they were calculated

Our web collection on [statistics for biologists](#) contains articles on many of the points above.

Software and code

Policy information about [availability of computer code](#)

Data collection NEX-GDDP CMIP6 climate data were downloaded using a custom-written code in R version 4.0.3. available at figshare (doi.org/10.6084/m9.figshare.16641079).

Data analysis Data analysis was performed in R version 4.0.3. The codes used in the analysis are available at figshare (doi.org/10.6084/m9.figshare.16641079).

The R session info and package used are provided below.
R version 4.0.3 (2020-10-10)
Platform: x86_64-pc-linux-gnu (64-bit)
Running under: Oracle Linux Server 8.3

Matrix products: default
BLAS: R/lib64/R/lib/libRblas.so
LAPACK: R/lib64/R/lib/libRlapack.so

locale:
LC_CTYPE=en_US.UTF-8; LC_NUMERIC=C; LC_TIME=en_US.UTF-8; LC_COLLATE=en_US.UTF-8; LC_MONETARY=en_US.UTF-8;
LC_MESSAGES=en_US.UTF-8; LC_PAPER=en_US.UTF-8; LC_NAME=C; LC_ADDRESS=C; LC_TELEPHONE=C; LC_MEASUREMENT=en_US.UTF-8;
LC_IDENTIFICATION=C.

attached base packages:

parallel; grid; stats; graphics; grDevices; utils; datasets; methods; base

other attached packages:

terra_1.4-22; bit_4.0.4; doParallel_1.0.16; Rmpi_0.6-9; data.table_1.14.0; doSNOW_1.0.19; snow_0.4-3; iterators_1.0.13; foreach_1.5.1; gmodels_2.18.1; weathermetrics_1.2.2; biclust_2.0.2; lattice_0.20-41; colorspace_2.0-0; MASS_7.3-53; exactextractr_0.6.0; dplyr_1.0.4; stringr_1.4.0; gdata_2.18.0; sf_0.9-8; raster_3.4-13; sp_1.4-5

loaded via a namespace (and not attached):

gttools_3.8.2; modeltools_0.2-23; tidyselect_1.1.0; purrr_0.3.4; flexclust_1.4-0; vctrs_0.3.6; generics_0.1.0; stats4_4.0.3; rlang_0.4.10; e1071_1.7-8; pillar_1.4.7; glue_1.4.2; DBI_1.1.1; lifecycle_1.0.0; munsell_0.5.0; gtable_0.3.0; codetools_0.2-16; class_7.3-17; Rcpp_1.0.7; KernSmooth_2.23-17; scales_1.1.1; classInt_0.4-3; additivityTests_1.1-4; ggplot2_3.3.3; stringi_1.5.3; tools_4.0.3; magrittr_2.0.1; proxy_0.4-26; tibble_3.0.6; crayon_1.4.1; tidyr_1.1.2; pkgconfig_2.0.3; ellipsis_0.3.1; assertthat_0.2.1; R6_2.5.0; units_0.7-2; compiler_4.0.3

For manuscripts utilizing custom algorithms or software that are central to the research but not yet described in published literature, software must be made available to editors and reviewers. We strongly encourage code deposition in a community repository (e.g. GitHub). See the Nature Portfolio [guidelines for submitting code & software](#) for further information.

Data

Policy information about [availability of data](#)

All manuscripts must include a [data availability statement](#). This statement should provide the following information, where applicable:

- Accession codes, unique identifiers, or web links for publicly available datasets
- A description of any restrictions on data availability
- For clinical datasets or third party data, please ensure that the statement adheres to our [policy](#)

NEX-GDDP CMIP6 climate data layer for the five GCMs were obtained from the NEX-GDDP CMIP6 webpage (nccs.nasa.gov/services/data-collections/land-based-products/NEX-GDDP-CMIP6; accessed January 2022). NEX-GDDP CMIP5 climate data layer for the five GCMs were obtained from amazon web services (data.nasa.gov/Earth-Science/Amazon-Web-Services-NASA-Earth-Exchange-NEX-Global/7yme-6yjr; accessed November 2020). Climate data for the low emission scenario were downloaded from the original CMIP6 runs (coarse resolution) from the Copernicus Climate Data Store (cds.climate.copernicus.eu; accessed January 2022). ECMFW ERA5 data was obtained from Copernicus Climate Data Store (cds.climate.copernicus.eu; accessed November 2020). Species distribution data are available for mammals and amphibians from IUCN (iucn.org; accessed November 2020), birds from BirdLife International (birdlife.org; accessed November 2020); reptiles from GARD initiative (doi.org/10.5061/dryad.9cnp5hqmb; accessed November 2020). Physiological thermal tolerance data were obtained from the GlobTherm database (doi.org/10.1038/sdata.2018.22; accessed November 2020).

Human research participants

Policy information about [studies involving human research participants and Sex and Gender in Research](#).

| | |
|-----------------------------|---|
| Reporting on sex and gender | <input type="text" value="Not applicable"/> |
| Population characteristics | <input type="text" value="Not applicable"/> |
| Recruitment | <input type="text" value="Not applicable"/> |
| Ethics oversight | <input type="text" value="Not applicable"/> |

Note that full information on the approval of the study protocol must also be provided in the manuscript.

Field-specific reporting

Please select the one below that is the best fit for your research. If you are not sure, read the appropriate sections before making your selection.

Life sciences Behavioural & social sciences Ecological, evolutionary & environmental sciences

For a reference copy of the document with all sections, see nature.com/documents/nr-reporting-summary-flat.pdf

Ecological, evolutionary & environmental sciences study design

All studies must disclose on these points even when the disclosure is negative.

| | |
|-------------------|---|
| Study description | <input type="text" value="Global assessment of land vertebrates' exposures to future extreme thermal events"/> |
| Research sample | <input type="text" value="Species geographic range data and daily climate data from 1950 to 2099"/> |
| Sampling strategy | <input type="text" value="All relevant data were used. No statistical methods were used to predetermine sample size."/> |
| Data collection | <input type="text" value="Data were based on existing datasets and was collected online by the authors."/> |

| | |
|--------------------------|--|
| Timing and spatial scale | Global data since 1950 to 2099 |
| Data exclusions | No data were excluded from the analyses |
| Reproducibility | This is not an experimental study, thus experimental replication was not performed |
| Randomization | Not applicable |
| Blinding | Not relevant, since this study is not experimental |

Did the study involve field work? Yes No

Reporting for specific materials, systems and methods

We require information from authors about some types of materials, experimental systems and methods used in many studies. Here, indicate whether each material, system or method listed is relevant to your study. If you are not sure if a list item applies to your research, read the appropriate section before selecting a response.

Materials & experimental systems

Methods

| n/a | Involvement in the study |
|-------------------------------------|--|
| <input checked="" type="checkbox"/> | <input type="checkbox"/> Antibodies |
| <input checked="" type="checkbox"/> | <input type="checkbox"/> Eukaryotic cell lines |
| <input checked="" type="checkbox"/> | <input type="checkbox"/> Palaeontology and archaeology |
| <input checked="" type="checkbox"/> | <input type="checkbox"/> Animals and other organisms |
| <input checked="" type="checkbox"/> | <input type="checkbox"/> Clinical data |
| <input checked="" type="checkbox"/> | <input type="checkbox"/> Dual use research of concern |

| n/a | Involvement in the study |
|-------------------------------------|---|
| <input checked="" type="checkbox"/> | <input type="checkbox"/> ChIP-seq |
| <input checked="" type="checkbox"/> | <input type="checkbox"/> Flow cytometry |
| <input checked="" type="checkbox"/> | <input type="checkbox"/> MRI-based neuroimaging |